

Contents lists available at ScienceDirect

Geoderma

journal homepage: www.elsevier.com/locate/geoderma





Mineral organic carbon interactions in dry versus wet tundra soils

Arthur Monhonval^a, Elisabeth Mauclet^a, Catherine Hirst^a, Nathan Bemelmans^a, Elodie Eekman^a, Edward A.G. Schuur^b, Sophie Opfergelt^{a,*}

- a Earth and Life Institute, Université Catholique de Louvain, Louvain-la-Neuve 1348, Belgium
- ^b Center for Ecosystem Society and Science, Northern Arizona University, Flagstaff, AZ, USA

ARTICLE INFO

Handling Editor: Alberto Agnelli.

Keywords:
Permafrost
Thawing
Mineral-associated organic carbon
Metal complexation
Eight Mile Lake

ABSTRACT

Mineral organic carbon interactions (aggregation, organo-mineral associations and organo-metallic complexes) enhance the protection of organic carbon (OC) from microbial degradation in soils. The northern circumpolar permafrost region stores between 1,440 and 1,600 Pg OC of which a significant portion is already thawed or about to thaw in coming years. In the light of this tipping point for climate change, any mechanism that can promote OC stabilization and hence mitigate OC mineralization and greenhouse gas emissions is of crucial interest. Here, we study interactions between metals (Fe, Al, Mn and Ca) and OC in the moist acidic tundra ecosystem of Eight Mile Lake, near Healy, AK, USA. We collected thirteen cores (124 soil samples) in late summer 2019 with shallow and deep active layers (45 to 109 cm deep) and varying water table depths. We find that between 6% and 59% of total OC in Eight Mile Lake tundra soils is mineral-associated (mean 20%), in organomineral associations (association between poorly crystalline oxides and OC) and in organo-metallic complexes (associations between Fe, Mn, Al, Ca polyvalent cations and organic acids). We find that total Fe and Mn concentrations can be used as good proxies to assess the reactive pool of these metals able to form associations with OC, i.e., poorly crystalline oxides or metals complexed with OC. We observe that in the active layer, mineral OC interactions are mostly as organo-metallic complexes with Fe cations, with an accumulation at the water table level acting as a soil redox interface. In waterlogged soils with a water table level above surface, no such accumulation of OC-Fe complexes is found due to the absence of a redox interface below soil surface. In the permafrost layer, we find that a combination of complexed metals and poorly crystalline Fe oxides act as reactive phases towards OC. Knowing that upon permafrost thaw tundra soils will become wetter or drier, the assessment of mineral-bound OC in drier or wetter tundra soils is a needed step to better constrain the changes in the proportion of non-protected OC more likely to contribute to C emissions from tundra soils.

1. Introduction

The permafrost region occupies about 22%-24% of the exposed land surface of the Northern Hemisphere (Brown et al., 1998; Obu et al., 2019; Zhang et al., 1999). The soil organic carbon (OC) stored in the northern circumpolar permafrost region is estimated to be 1440–1600 Pg C, in surface and deeper (>3 m) soil layers (Hugelius et al., 2014; Schuur et al., 2015; Strauss et al., 2017). Rising temperatures, two times more rapid in northern regions compared to global warming, result in the gradual thaw of permafrost, i.e., deepening of the soil layer that thaws every summer, referred as the active layer thaw (Luo et al., 2016; Schuur et al., 2015). Permafrost thaw is a major tipping point in the climate system (IPCC, 2021; Lenton et al., 2019) because of its climate-sensitive OC pool under threat of being transferred to the atmosphere as

greenhouse gases carbon dioxide (CO₂) and methane (CH₄) upon microbial degradation (Schuur et al., 2013, 2008; Zimov et al., 2006).

The impact of climate warming on the hydrology of northern permafrost soils is complex (Bring et al., 2016; Vonk et al., 2019). Permafrost tundra soils are expected to be drier with increasing evapotranspiration and drainage as a consequence of permafrost thaw (Avis et al., 2011; Bring et al., 2016). However, local increases in water saturation in soils are predicted in areas that collapse and fill with water because of the impermeable permafrost table that prevents drainage (Swindles et al., 2016). Waterlogged soils face major changes in biogeochemical conditions (Kögel-Knabner et al., 2010): the presence of the water table at the surface restricts oxygen diffusion which lowers the reductive-oxidative (redox) potential and promotes metal oxides dissolution or anaerobic processes (such as methane production). Most

E-mail address: sophie.opfergelt@uclouvain.be (S. Opfergelt).

^{*} Corresponding author.

permafrost-affected ecosystems suffer from periodic or persistent anoxia due to soil water saturation (Street et al., 2016).

The mechanisms of OC stabilization involving mineral OC interactions, i.e., the mineral protection of OC, are highly dependent on the soil moisture and hence redox state of tundra soils (Bhattacharyya et al., 2018a; Fiedler and Sommer, 2004; Herndon et al., 2020; Winkler et al., 2018). While the importance of such interactions for OC protection has been assessed in many environments, from temperate, forest and volcanic soils to paddy soils and marine sediments (e.g., Eglinton, 2012; Eusterhues et al., 2005; Inagaki et al., 2020; Kalbitz and Kaiser, 2008; Lalonde et al., 2012; Masiello et al., 2004; Mikutta et al., 2007; Pan et al., 2014; Wang et al., 2019), the focus on permafrost soils is only recently growing (Fiedler et al., 2004; Herndon et al., 2020, 2017; Joss et al., 2022; Monhonval et al., 2021a; Mu et al., 2016; Patzner et al., 2020; Wang et al., 2021). Our understanding on the changes of mineral OC interactions between drier and wetter tundra soils remains incomplete, particularly with respect to changing water saturation in the active layer upon thawing.

Mineral OC interactions result in the protection of OC from degradation via aggregation, organo-mineral associations and organometallic complexes (Baldock and Skjemstad, 2000; Kleber et al., 2015; Torn et al., 1997; von Lützow et al., 2006). Aggregation offers physical protection whereas organo-mineral associations and organo-metallic complexes offer physico-chemical protection of OC. In aggregates, OC is occluded in the tridimensional arrangement of minerals involving metal oxides (e.g., goethite, hematite, ferrihydrite, birnessite), limiting the access for microorganisms to the trapped OC. Organo-mineral associations involve the ligand exchange (alongside other binding mechanisms) between OC and phyllosilicates or metal oxide surfaces, which are among the most effective sorbent for dissolved OC (e.g., Kaiser et al., 1997; Stumm, 1992). In organo-metallic complexes, metals (i.e., Fe^{3+/} $^{2+}$, Al^{3+} , $\mathrm{Mn}^{3+/2+}$ or Ca^{2+}) act as polyvalent cations and coordinate to the functional groups of organic acids (e.g., Boudot et al., 1989). In organo-mineral associations and organo-metallic complexes, OC is less soluble and therefore less available for microorganisms which contributes to mitigate greenhouse gas emissions from permafrost soils.

We hypothesize that soil moisture content is a major player in controlling mineral OC interactions in moist acidic tundra soils. Indeed, in poorly drained organic-rich soils well represented in moist acidic tundra soils, soluble Fe²⁺ present in the mineral horizons can migrate to more oxic zones and accumulate as a mixture of organic-bound (i.e., complexed) Fe²⁺ and Fe³⁺, and Fe oxy(hydr)oxides (Bhattacharyya et al., 2018b; Herndon et al., 2017; Lipson et al., 2012; Riedel et al., 2013), thereby contributing to form mineral OC interactions. In contrast, in waterlogged soils, such accumulation of complexed Fe and Fe oxy(hydr) oxides is less likely. In the absence of oxic conditions within the soil profile, due to the high soil moisture content, soil redox potential decreases and in turn may increase oxide dissolution and release previously stabilized OC, hence increasing OC vulnerability to mineralization (Lipson et al., 2012). In addition to the major role of redox conditions, we also hypothesize that mineral OC interactions differ with changing pH conditions between organic-rich surface horizons and mineral-rich deeper soil horizons (Parkinson, 1978; Ping et al., 2005). The soil pH controls oxides dissolution rates and can protonate or deprotonate organic acids functional groups or oxide surfaces, modifying organic acids-oxides association (Kleber et al., 2021; Kleber et al., 2015; Pan et al., 2014). A shift in pH would change the relative importance of Fe, Al versus Ca metal as polyvalent cations participating in complexation (Rowley et al., 2018). Finally, we hypothesize that with permafrost thaw, additional mineral and OC stored in frozen layers will become available to form mineral OC interactions (Hirst et al., 2022; Opfergelt, 2020).

Testing these hypotheses requires a better understanding on the dynamics of Fe, Al, Mn and Ca and their interactions with organic acids in permafrost soil ecosystems. Here, we investigate the proportion of mineral OC interactions (including Fe, Al, Mn and Ca with a particular

focus on Fe) in a range of dry and wet tundra soils. We study 13 profiles with varying active layer and water table depths from a well described moist acidic tundra site near Eight Mile Lake, Healy, AK, USA. We determine the total pool of Fe, Al, Mn and Ca and quantify the reactivity of these metals with OC.

2. Material and methods

2.1. Site description and soil sampling

Soil profiles were collected at Gradient site from the Eight Mile Lake (EML) watershed in a moist acidic tundra located near Healy, Alaska, USA (63.87°N; 149.25°W, 700 m elevation, Fig. 1a) in late summer 2019, at the time of deepest active layer thaw. Gradient site is a natural gradient of permafrost thaw and thermokarst development (i.e., gullies and water tracks) monitored for ~40 years (Osterkamp et al., 2009; Schuur et al., 2009). Mean annual air temperature averaged -0.94 °C from 1977 to 2015 with a non-summer (October-April) average of -10.09 °C and summer (May-September) average of 11.91 °C (Healy and McKinley Stations, Western Regional Climate Center and NOAA National Centers for Environmental Information) (Mauritz et al., 2017). Permafrost is close to thaw because its temperature approximates the mean annual air temperature of -1° C (Osterkamp and Romanovsky, 1999) and is still rising (Osterkamp et al., 2009). Soils are Histic Turbic Cryosols (IUSS Working Group WRB, 2015). The area is characterized with peat accumulations (up to 40 cm) over fine-grained soils of loess origin associated with colluvial deposits. The upper 1 m of soils at Eight Mile Lake have characteristically high moisture content, within 48% 60% by volume in 2009, and thus are highly vulnerable to the formation of thermokarst terrain (Garnello et al., 2021; Osterkamp et al., 2009). The Gradient site was historically determined based on increase subsidence and thaw settlements downslope previously referred as Minimal (Min), Moderate (Mod) and Extensive (Ext) thaw (Osterkamp et al., 2009). Windblown snow fills thermokarst depressions causing further warming and thawing of the underlying permafrost (Osterkamp et al., 2009). The thermokarst development at Eight Mile Lake has initiated a shift in vegetation cover, with evergreen and deciduous shrubs and forbs becoming dominant at the expense of tussock forming sedges in drier sites, and sedges and mosses being dominant in wetter sites (Mauclet et al., 2022; Natali et al., 2011; Schuur et al., 2007; Villani et al., 2022). Long-term monitoring at the Gradient site (between 2004 and 2021) supports the spatial and temporal change in active layer and water table depth with ongoing permafrost thaw (Kelley et al., 2022; Schaedel et al., 2022; Schuur et al., 2021), shifting from the originally defined thaw gradient.

Thirteen soil profiles were sampled to include sites from the originally defined Gradient site (Min, Mod, Ext), and also sites well drained (Dry or partially unsaturated), poorly drained (Wet), waterlogged (Pond), and with preferential water flow path (Water track) (Fig. 1b). The upper part of the soil profiles (up to 45 cm) were collected using chisel and knife in 5 cm increments which prevented compaction within organic-rich layers. Below the water table, cores were retrieved using a stainless-steel pipe (diameter 44 mm) which was manually hammered down into active layer and permafrost (Fig. 1c). The core within the steel pipe was subdivided in 10 cm increments. Note that compaction in the surface layers of water-saturated soils (i.e., especially ponds and water track profiles) was inevitable using the steel pipe method. This study presents 13 soil profiles combining a total of 124 samples from poorly thawed profiles (active layer depth <60 cm; profiles by increasing active layer depth: Dry $5 < Ext \ 1 < Mod \ 1 < Min \ 1 < Pond \ 10 < Min \ 3)$ and deeply thawed profiles (active layer depth > 60 cm; profiles by increasing active layer depth: Pond $1 < Ext \ 3 < Mod \ 3 < Pond \ 9 < Mod$ 2 < Wet 4 < Watertrack 1) (Fig. 1b; Table S1). The 60 cm limit is representative of the modern day active layer reported in EML soils (Hutchings et al., 2019). Within the 13 profiles, active layer depth ranged between 45 and 109 cm b.s. (below surface, i.e., below the

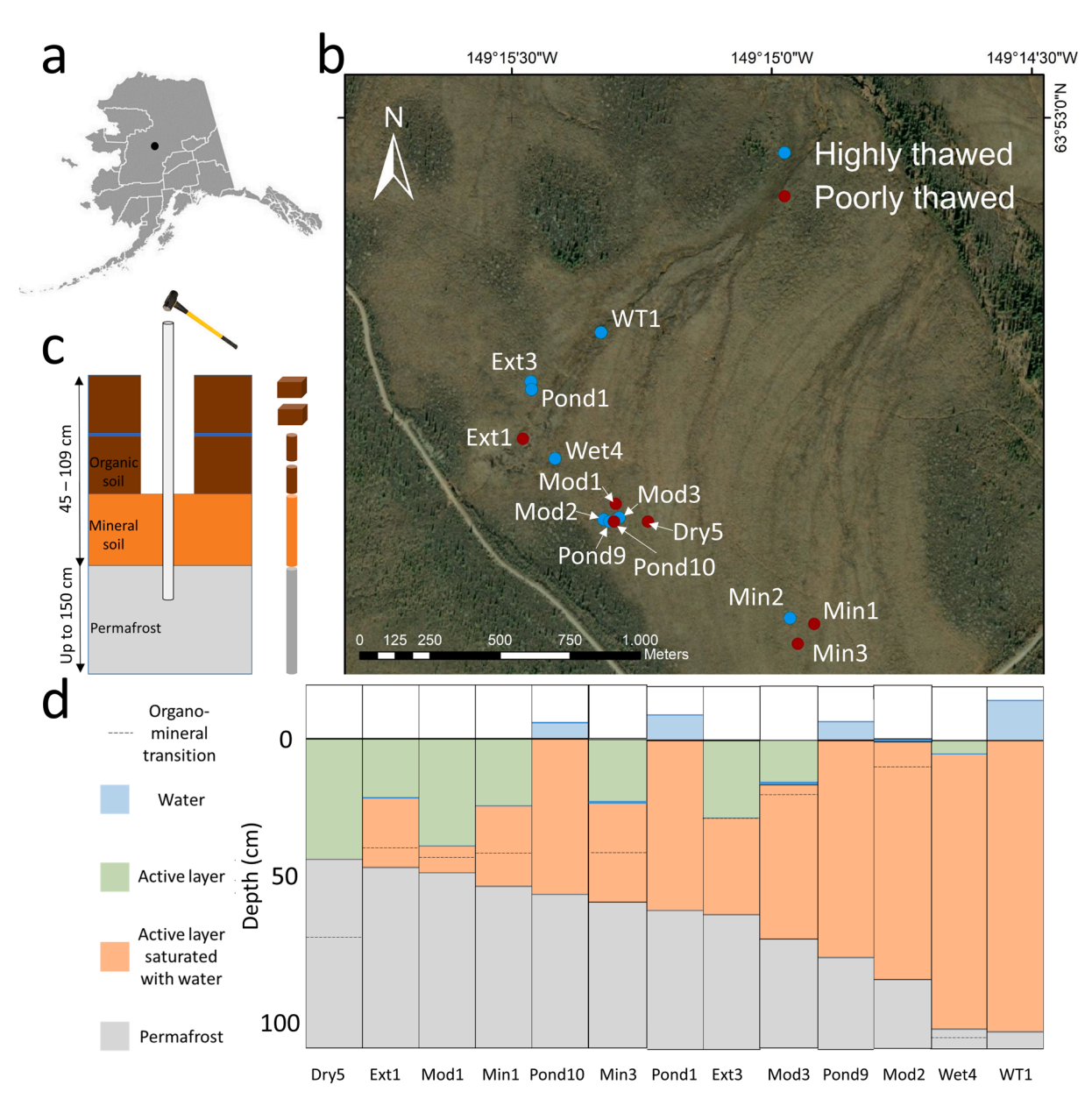


Fig. 1. (a) Location of Eight Mile Lake Gradient site near Healy, Alaska, USA. (b) Coring locations within the Gradient site for the thirteen soil profiles including poorly (active layer depth <60 cm; brown) and deeply (active layer depth >60 cm; blue) thawed profiles (Table S1). (c) Sampling scheme with chisel and knife above the water table and steel pipe hammered down into active layer and permafrost below the water table (blue line = water table position). (d) Stratigraphic representation of active layer and water table depth for the thirteen soil profiles.

aboveground part of the vegetation) and water table depth between 45 cm b.s. and 15 cm a.s. (above surface) (Table S1). Permafrost was reached for all 13 profiles to a maximum depth of 150 cm. In total, this study presents 73 samples from active layer soils and 51 from permafrost layers (n = 64 samples from poorly thawed soil profiles; n = 60 from deeply thawed soil profiles). All samples were air dried in the laboratory. Samples from the litter (0–5 cm layer) were shredded without anterior sieving while other samples were sieved at 2 mm and ground prior to laboratory analyses.

2.2. Measurements of total concentrations in metals (Fe, Mn, Al and Ca) and organic carbon

We assessed total Fe, Mn, Al and Ca concentrations using a portable X-ray fluorescence (pXRF) device ($Niton^{TM}$ XL3t GOLDD+, Thermo Fisher Scientific, Waltham, USA) following the method described fully in Monhonval et al. (2021b). The pXRF method needs to be calibrated to

ensure trueness. We compared the total metal concentrations measured by pXRF with metal concentrations obtained using inductively coupled plasma optical-emission spectrometry (ICP-OES; iCAP 6500 Thermo Fisher Scientific) after sample dissolution by alkaline fusion (Chao and Sanzolone, 1992). The loss on ignition at 1,000 °C allows to verify the sum of oxides (between 98 and 102%). Total elemental content is expressed in reference to the soil dry weight at 105 °C. We performed pXRF and ICP-OES measurements on 39 samples from Gradient site in addition to the 144 samples based on the work from Monhonval et al. (2021b) on ice-rich permafrost samples. We observed that two corrections were needed depending on total organic carbon (TOC) content. The pXRF measurement involves X-ray beam penetration of the sample and fluorescence energy needs to be detected back by the pXRF device. The density of the sample (i.e., the amount of air present in the porosity of the sample) may cause under estimation of metal concentration, hence correction to ensure trueness is needed (Ravansari et al., 2020; Ravansari and Lemke, 2018). Samples with lower TOC content (<20 wt

%), considered as mineral matrix, followed the linear regression previously assessed in Monhonval et al. (2021b) (Fig. S1). Samples with higher TOC content (>20 wt%) displayed another linear regression and therefore need to be corrected using another equation for Fe, Mn and Ca, whereas only one linear regression was necessary for Al ($\rm R^2=0.91$). The coefficient of variation (i.e., CV, the ratio of the standard deviation to the mean concentration) of the pXRF method equals 0.74% (Fe), 3.7% (Al), 2.9% (Mn), 0.84% (Ca), and for ICP-OES method 0.50% (Fe), 0.43% (Al), 0.85% (Mn) and 0.99% (Ca) (Monhonval et al., 2021b).

The TOC content was derived from the total soil carbon content measured on all samples (n = 124) with a Vario El cube elemental analyzer (Elementar, Langensebold, Germany). About 5–7 mg of sample was used by measurement, and each sample was weighed and processed twice for carbon analysis to calculate a mean value. The average standard deviation for C content is $\sim\!5\%$ and the detection limit is $<\!0.1\%$. Total C measurements are expressed as weight percentage (i.e., wt%) in reference to the soil dry weight at 105 °C. With no presence of carbonates detected, the total soil carbon content is considered equivalent to the TOC content.

2.3. Selective extractions of metals (Fe, Mn, Al and Ca) and organic acids

Selective extractions of Fe, Mn, Al and Ca were performed on all samples (n = 124) using i) dithionite-citrate-bicarbonate (DCB), ii) ammonium oxalate in the dark for 4 h, and iii) Na-pyrophosphate for 16 h. The DCB extraction is presumed to remove oxides (well and poorly crystalline oxides) as well as complexed (i.e., organic-bound) metals (Mehra and Jackson, 1960). The ammonium oxalate in the dark extraction (in the following referred as oxalate extraction) is presumed to remove poorly crystalline oxides and complexed metals (Blakemore et al., 1981). This oxalate extracted pool will be defined as the reactive metals because of their high reactivity to bind with OC. The Napyrophosphate extraction is presumed to remove only organically complexed metals and also dispersible colloids (Bascomb, 1968; Parfitt and Childs, 1988). These extractions are not fully quantitative and some dissimilarities between the theoretical and practical extracted pool may appear (Rennert, 2019). However, these are commonly used extraction methods that can be used as indicators of the oxides and complexed pools within a particular soil. The amount of well crystalline Fe oxides is calculated as the difference between DCB- and oxalate-extracted Fe (i.e., Fed - Feo), and the amount of poorly crystalline Fe oxides (i.e., ferrihydrite) by the difference between oxalate and pyrophosphate-extracted Fe (i.e., Fe₀ - Fe_p). The same can be done for Mn but not Al for which DCB extraction do not target Al oxides specifically (Rennert, 2019). Note that Ca concentration within the oxalate extraction is not relevant given that Ca oxalate precipitates and does not remain in solution for ICP-OES measurement. Metal concentrations (Fe, Mn, Al and Ca) in the extracts were analyzed by ICP-OES (iCAP 6500 Thermo Fisher Scientific) and are expressed in reference to the soil dry weight at 105 $^{\circ}$ C (mg kg⁻¹). The limit of quantification (LOQ) was reached for oxalate-extracted Mn ($<0.008 \text{ mg L}^{-1}$, corresponding to 6 mg kg $^{-1}$ in solid sample) for 30 out

Organic acids were analyzed using indirect or direct measurements within the oxalate extract and the pyrophosphate extract, respectively. Note that the organic composition of the DCB and oxalate solutions do not allow direct measurement of OC. The optical density of oxalate extract (ODOE), considered as an indicator of reactive polyaromatic acid concentration, was measured by determining the absorbance at 430 nm on a Genesys 10 S VIS spectrophotometer, with the ammonium oxalate reagent as a blank (Daly, 1982). From the pyrophosphate extract, the concentration in dissolved OC released after dispersion by pyrophosphate (referred as C_p) was measured using a Shimadzu TOC-L Analyzer (measuring non purgeable OC; LOQ = 0.1 mg L⁻¹; accuracy $\pm 2\%$). This indicates the amounts of C participating in organo-metallic complexes in soils (Bascomb, 1968). The LOQ was never reached for any samples.

2.4. Statistical analysis

Correlation analysis using Pearson method between metal and organic parameters were constructed using *corrplot* package. To assess statistical differences between two datasets, we performed the Wilcoxon test. All statistics were performed using R core software (R Core Team, 2018). All data values are available in Supplementary Material Data.

3. Results

3.1. Total and selectively extracted metals (Fe, Mn, Al and Ca) in permafrost tundra soils

The metal concentrations (Fe, Mn, Al and Ca) are presented for a partially unsaturated profile which is poorly thawed (i.e., dry; Min 3) and a waterlogged profile which is deeply thawed (i.e., wet; Mod 2) (Fig. 2) as a function of their water table depth and active layer depth. Considering the distance to the water table, the trends observed for the reactive metal concentrations (oxalate-extracted Fe, Mn, Al, and pyrophosphate-extracted Ca) are compared within the thirteen soils profiles studied (Fig. 3; Fig. S2).

In the partially unsaturated soils studied (i.e., when water table is below the soil surface), Fe is the only metal that accumulates at the water table level for both the total and selectively extracted concentrations (Fig. 2; Fig. 3; Fig. S2). In most of the partially unsaturated soils, the total Mn concentration is high in the litter horizon (0–5 cm layer), decreases within the organic layer and increases within the mineral soil (Fig. S2). Selectively extracted Mn is in the high range of values within the litter and in the low range values in the remaining of the profile (except in the deepest samples where Mn accumulation is observed; Fig. 2b; Fig. 3). In partially unsaturated soils, total Al concentrations are higher in the mineral soil (e.g., below 30 cm in profile Min 3) compared to the organic-rich soils (e.g., above 30 cm in profile Min 3; Fig. 2c; Fig. S2). Selectively extracted Al concentrations are lower in organic and permafrost samples compared to mineral samples from the active layer (Fig. 2c; Fig. 3). Similarly in partially unsaturated soils, total Ca concentrations are high in mineral and low in organic layers but the opposite is observed for complexed (i.e., pyrophosphate extracted) Ca (Fig. 3; Fig. S2). The difference between total and complexed Ca concentrations are low in organic-rich soils but the total Ca is one order of magnitude higher than the complexed Ca in mineral soils (Fig. S2).

In the waterlogged soils studied (where the water table depth is close to the surface), Fe accumulation at the water table depth and Mn accumulation in the litter horizons is limited or is absent (Fig. 2e and f; Fig. S2). Note that an accumulation of Fe and/or Mn concentration were observed in the permafrost layers of some waterlogged soil profiles (i.e., Min 3, Pond 9, Mod 3; Fig. 2; Fig. S2). Total and selective Al and Ca show the same trend for both partially unsaturated and waterlogged soils. In all profiles, DCB-extracted and oxalate-extracted Fe and Mn often overlap, which suggests no presence of well crystalline Fe or Mn-oxides (Fig. S2). In addition, for most of the soil profiles, pyrophosphate-extracted and oxalate-extracted Fe and Mn concentrations overlap within the organic active layer and differ within the permafrost layer (Fig. 2; Fig. S2).

3.2. Total organic carbon and organic acids in permafrost tundra soils

This section describes the total organic carbon content (TOC, in wt %), the optical density of the oxalate extract (ODOE, indicator of polyaromatic acids) and complexed (i.e., pyrophosphate extracted) C concentration based on two typical soil profiles, a partially unsaturated profile which is poorly thawed (i.e., dry; Min 3) and a waterlogged profile which is deeply thawed (i.e., wet; Mod 2), and the other profiles studied (Fig. S3).

The TOC content ranges between 0.7 and 49.7 wt% for all soil profiles (n = 124; Supplementary Material Data). The organo-mineral

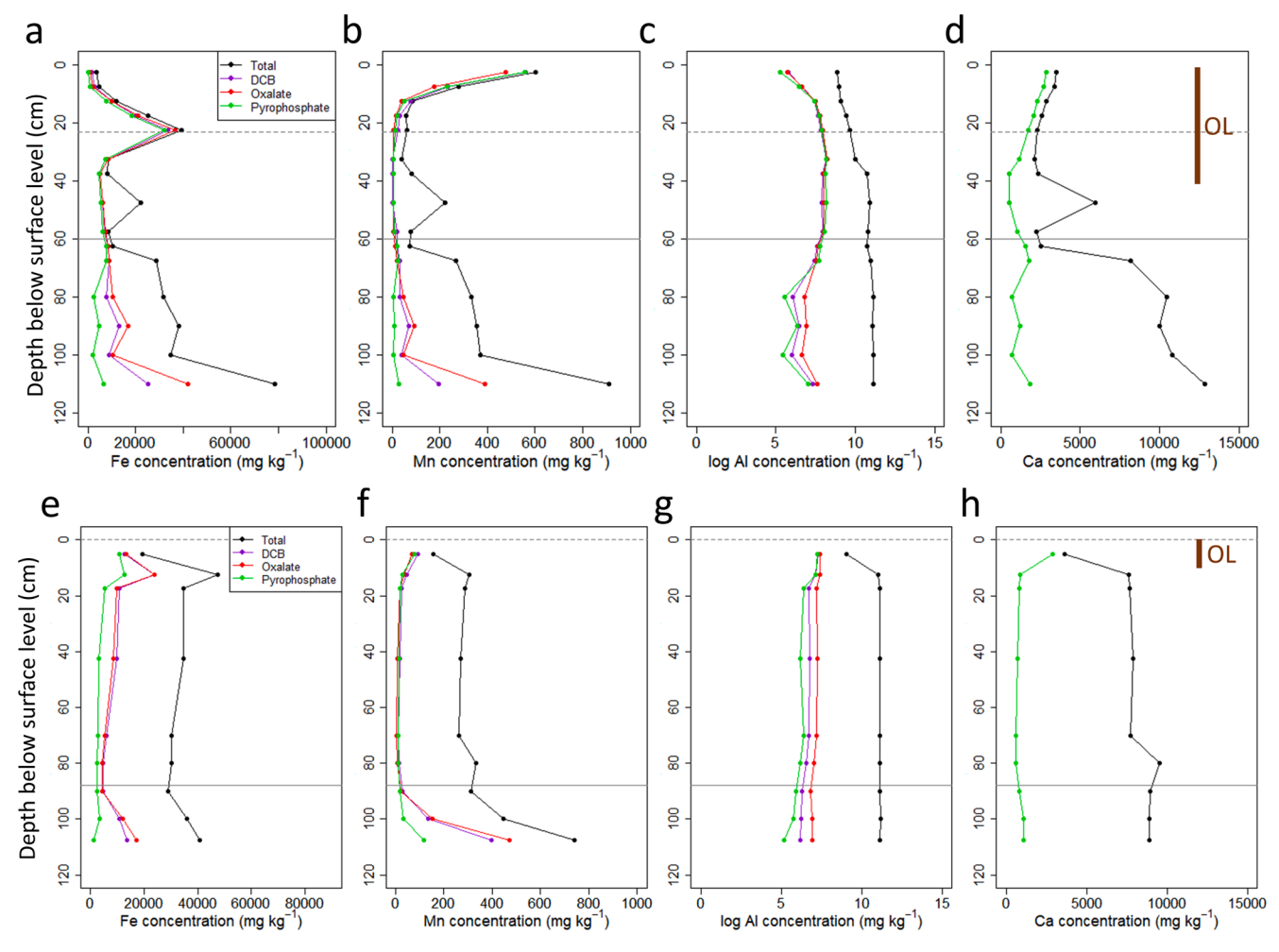


Fig. 2. Partially unsaturated poorly thawed soil profile (Min 3; a-d) and waterlogged deeply thawed soil profile (Mod 2; e-h) depth evolution of total metal concentrations and selectively extracted metals using dithionite-citrate-bicarbonate (DCB), ammonium oxalate (oxalate) and Na-pyrophosphate for (a) Fe, (b) Mn, (c) Al and (d) Ca. Dashed and continuous line represents the water table and permafrost table depth, respectively. A logarithmic scale is used for Al. The Ca is only represented for total and pyrophosphate concentrations. The organo-mineral transition (cut-off at 20 wt% TOC) is at 20 cm depth. The organic layer (OL) is represented on panel d (Min 3) and h (Mod 2).

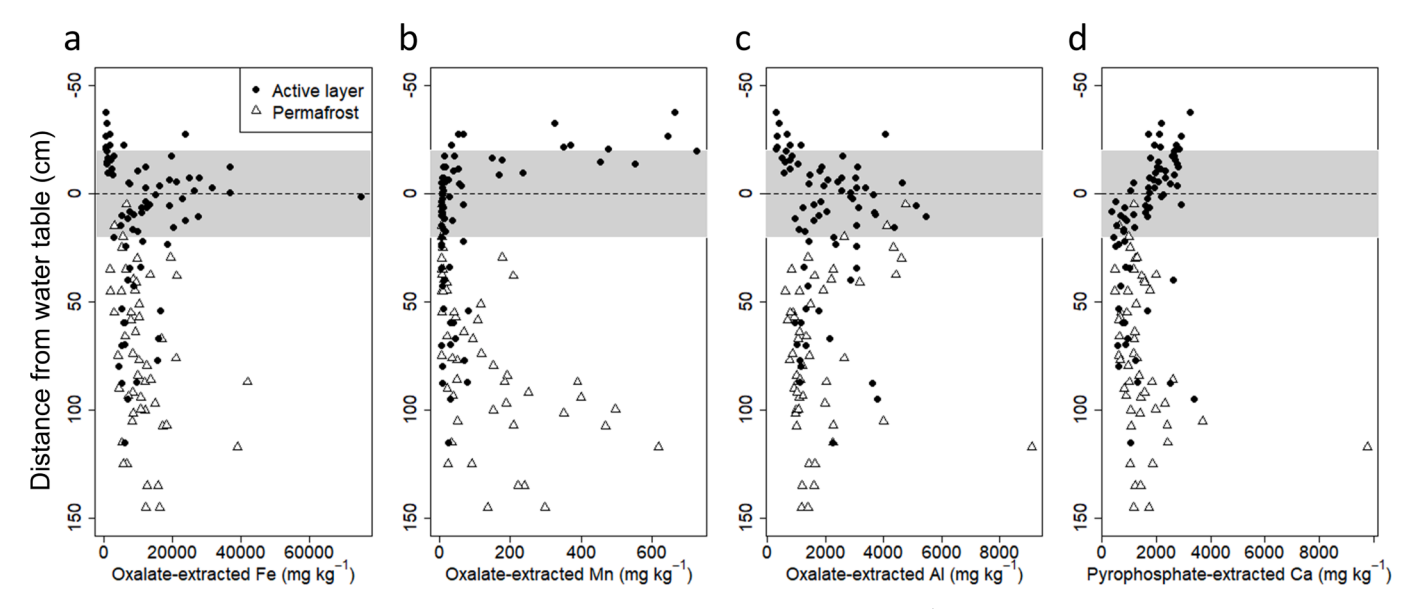


Fig. 3. Oxalate-extracted (a) Fe, (b) Mn, (c) Al and (d) pyrophosphate-extracted Ca concentration (mg kg^{-1}) as function of the distance of the sample to the water table in the thirteen soil profiles. The greyish rectangle represents samples from a distance smaller than 20 cm above or below water table. Samples from the active layer (unfrozen) and permafrost (frozen) are represented as black points and white triangles, respectively.

transition (i.e., where samples shift from TOC values higher than 20 wt% in organic horizons to TOC values lower than 20 wt% in mineral horizons) is generally found between 10 and 40 cm below surface. The organic samples present a mean of 40 wt% TOC and mineral samples of 5 wt% TOC. The ODOE and the complexed C are well correlated (r=0.81). However, TOC content is poorly correlated with ODOE but better correlated with C_p (r = 0.36 and 0.73, respectively). The TOC content is high in the surface and decreases within the mineral horizons. Exceptionally, buried peat (organic-rich) layers were detected in some profiles (i.e., 34 wt% TOC at 110 cm in Pond 9, Fig. S3). The ODOE value increases at the water table level. Similarly, complexed C concentration accumulates at the water table level. This accumulation of ODOE and C_p values are sometimes found in buried frozen peat layers (Fig. 4 and Fig. S3). In waterlogged soils, such accumulation in ODOE or C_p value is not found within surface soils or with significantly lower values (Fig. 4d - f).

3.3. Correlation between reactive metals and organic carbon

A correlation matrix between all concentrations (total and

selectively extracted metals, total and selectively extracted C) is shown in Fig. S4. Correlation coefficients show that the higher negative correlation lies between total Al and TOC (r=-0.99). The highest positive correlation lies between DCB- and oxalate-extracted Fe (r=0.98) and DCB- and pyrophosphate extracted Al (r=0.99). Overall, total concentrations of each metal are positively correlated to their selective extracted concentrations. The TOC content is positively correlated with complexed Fe, Mn, Al and Ca ($r=0.38,\,0.39,\,0.41$ and 0.56, respectively) and with selectively extracted carbon (r=0.36 for ODOE and r=0.73 for C_p). All other parameters are negatively correlated or not correlated with TOC. The best correlation for ODOE is observed for selectively extracted Fe species (max correlation with Fe_p, r=0.94) as well as complexed C (r=0.81). Complexed C is positively correlated with selectively extracted Fe, Al and Ca but not correlated with selectively extracted Mn concentrations.

The overlap between the concentration of complexed and poorly crystalline minerals (oxalate extraction) and the concentration of complexed metals (pyrophosphate extraction) along the profiles (Fig. 2; Fig. S2) highlights that complexation largely contributes to mineral-associated OC (especially in active layer soils) in these moist acidic

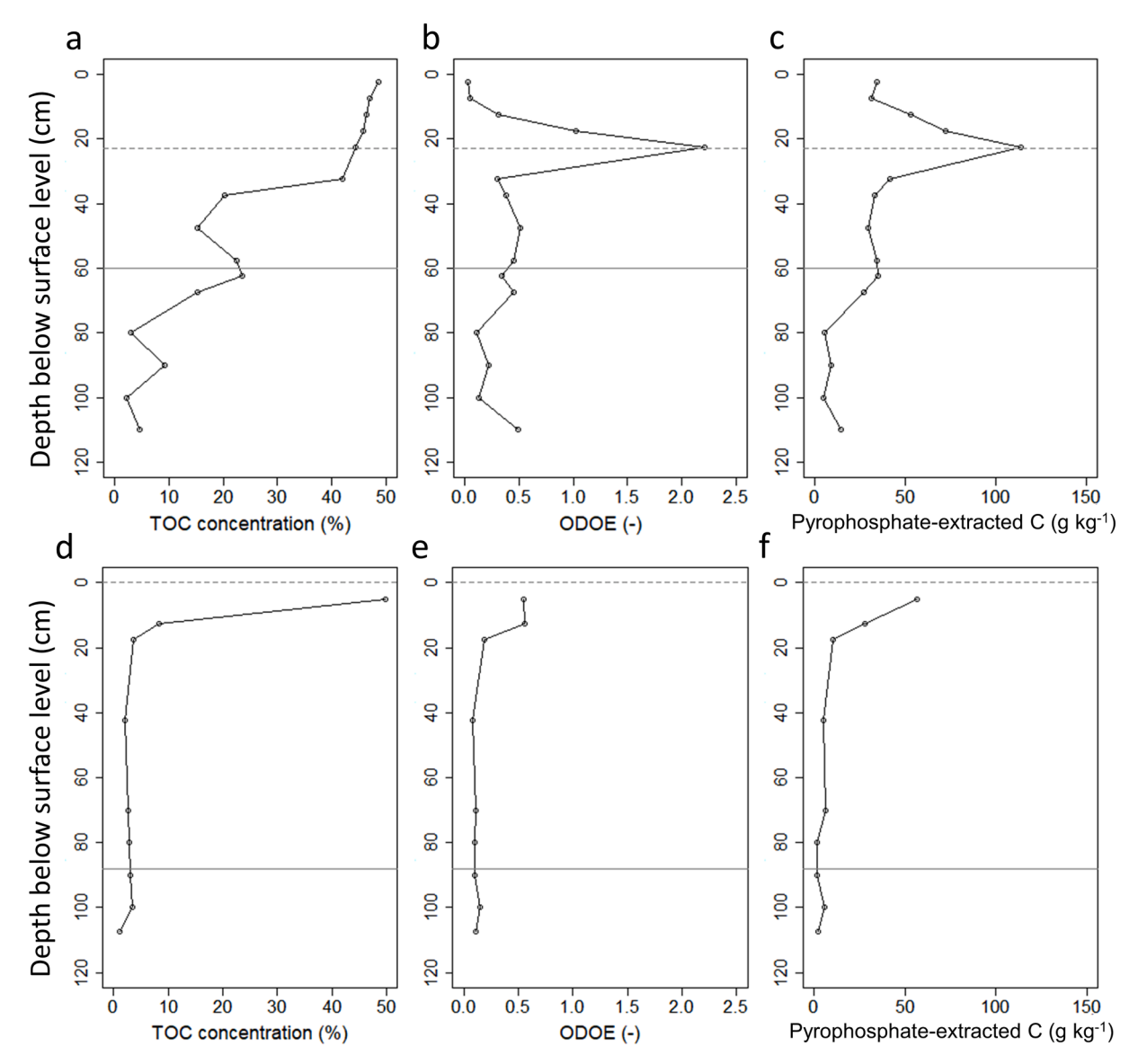


Fig. 4. Partially unsaturated poorly thawed profile (Min 3; a-c) and waterlogged deeply thawed profile (Mod 2; d-f) depth evolution of (a and d) total organic carbon (TOC) content (in %), (b and e) optical density of the oxalate extract (ODOE, adimensional), an indicator of organic acid concentration, and (c and f) pyrophosphate extracted C concentration (C_p , in g kg⁻¹). Dashed and continuous line represents the water table and permafrost table depth, respectively.

tundra soils (Table S2). More specifically, as illustrated for a poorly thawed (Min 3) and a deeply thawed (Mod 2) profile, metal cations (Fe, Al, Mn, Ca) coordinate with the functional groups of organic acids in various proportions (Fig. 5). In the top of the soil profile, within the litter, organo-metallic complexes are dominated by Ca (contributing to 63% of total complexed metals) but the Ca contribution to organomineral complexation decreases in deeper soil layers (Fig. 5a). Organic complexation with Mn is a minor contributor in the litter and is negligible compared to Fe, Al and Ca deeper in the soil profile. Organic complexation with Fe is dominant under unsaturated soil conditions

while complexation with Al increases under waterlogged and likely long-term saturated soil conditions (Fig. 5a and c). In most permafrost layers, Fe is the dominant polyvalent cation for complexation with OC (Fig. 5). On average, all samples combined (n = 124 from 13 profiles), the molar contribution of each metal to complexation is decreasing from Fe (48.4%), Ca (25.9%), Al (24.3%) and Mn (1.4%). Note that Ca contribution is high on average because of its dominant contribution in surface soils (up to 75% in the litter). The correlation between the sum of complexed metals and complexed carbon is high (r = 0.9), both accumulating at the water table depth (as illustrated for the poorly thawed

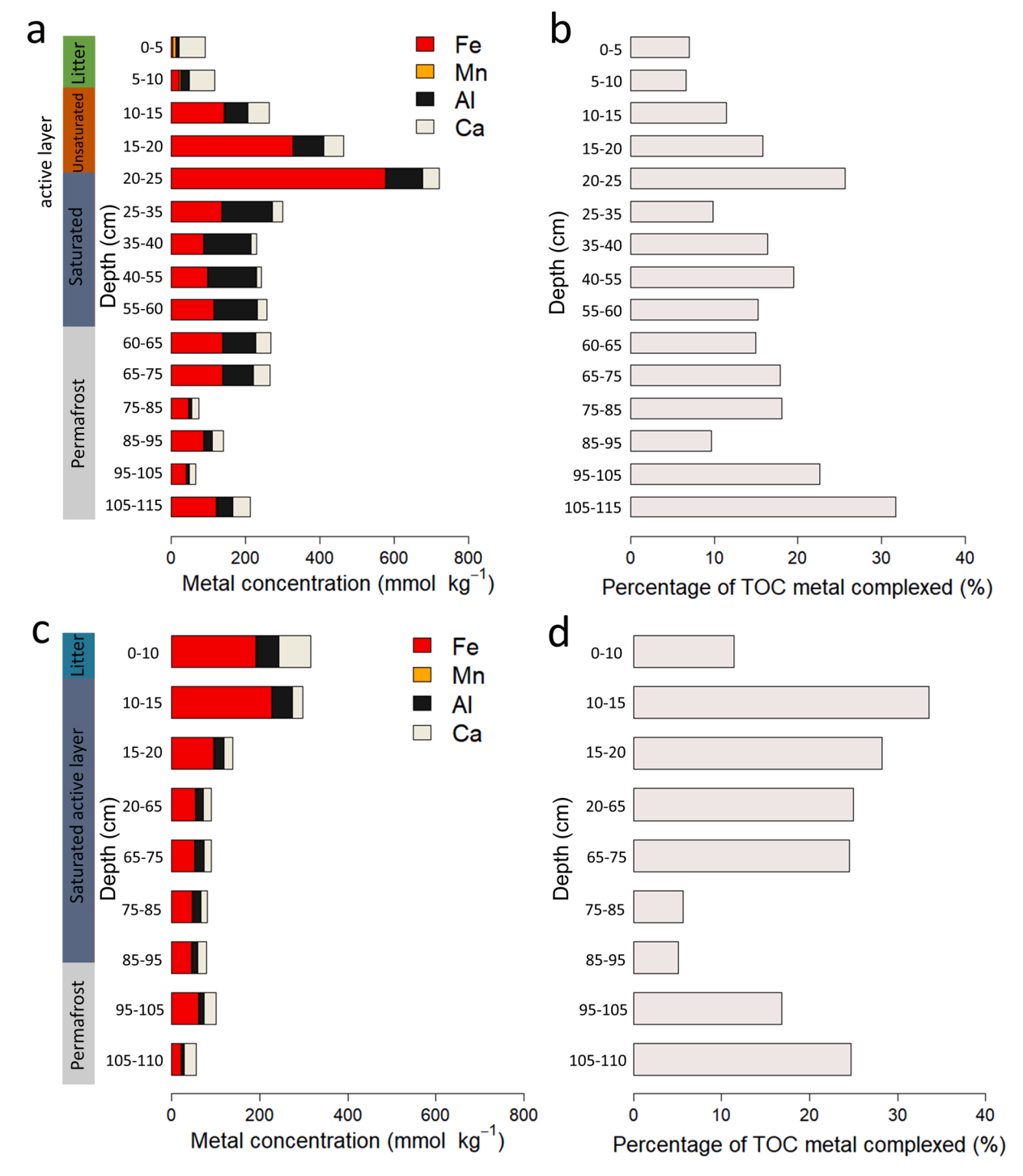


Fig. 5. For a partially unsaturated poorly thawed soil profile (Min 3; a-b) and waterlogged deeply thawed soil profile (Mod 2; c-d) profile: (a, c) Pyrophosphate-extracted metals (Fe, Mn, Al and Ca) in mmol kg⁻¹ and (b, d) percentage of total organic carbon (TOC) complexed with metals. The stratigraphic column on the left represents permafrost (gray), saturated (blue) and unsaturated (brown) active layer and litter (green).

profile Min 3; Fig. 4c and Fig. 5a).

Overall, between 5% and 35% of TOC is complexed to metals under dry and wet tundra soil conditions: this range is similar for poorly thawed and deeply thawed profiles, as illustrated for Min 3 (7%–32%) and Mod 2 (5%-34%), respectively (Fig. 5b – d). The concentration of complexed metals is higher in active layer soils (mean = 266 mmol kg $^{-1}$) compared to underlying permafrost layers (173 mmol kg $^{-1}$) (illustrated for Min 3 and Mod 2; Fig. 5a – c). However, the proportion of metal-complexed TOC is significantly higher in permafrost soils than in active layer soils (mean of 25.4% and 16.5%, respectively; p-value <0.01) due to the higher TOC content in the active layer (illustrated for Min 3 and Mod 2; Fig. 5b – d).

4. Discussion

4.1. Mechanisms of mineral OC interactions in tundra soils

4.1.1. Influence of water saturation and pH on metals involved in complexation in tundra soils

The positive correlation between the sum of the pyrophosphate-extracted metals and the pyrophosphate-extracted carbon (r=0.9; section 3.3; Fig. S4) indicates a large contribution of complexation as a mechanism of mineral OC interactions in these soils, as reported for permafrost peatlands (Lim et al., 2022). Here we discuss how soil properties (such as soil water saturation and soil pH) may influence complexation for the different metals investigated in this study (Fe, Mn, Al and Ca).

For a redox-sensitive element such as Fe, water saturation is a major control on its contribution to OC complexation. The accumulation of Fe-OC complexes at the water table (Fig. 2a, Fig. 3a), i.e., at the redox interface, results from lower Fe/DOC ratio in soil solution in saturated than in unsaturated conditions at the site (Hirst et al., 2022). Indeed, lower Fe/DOC ratio in soil solution promotes the formation of Fe-OC complexes (Jansen et al., 2003). Even if Mn is a redox sensitive element such as Fe, the contribution of Mn to OC complexation is not mainly driven by water saturation: Mn-OC complexes do not accumulate at the redox interface but in the litter horizon (0-5 cm soil layer). The organic layer is known to be enriched in Mn due to accumulation of Mn in the litter (Villani et al., 2022; Mauclet et al 2022): this likely contributes to a larger contribution of Mn to organo-metallic complexes in the litter horizon. This is consistent with the well-established Mn cycling through vegetation and accumulation in surface soils (Fiedler et al., 2004; Jobbágy and Jackson, 2004; Li et al., 2021).

Even if OC complexation with Fe is dominant, Al complexation may increase and contribute equally or more than Fe complexation in some persistent water-saturated or permafrost layers (deeper mineral layers). As illustrated for Min 3, the contribution of Al complexation reaches 61% at 35-55 cm depth, i.e., at the bottom of the active layer in saturated conditions (WTD = 25 cm b.s.; Fig. 5a). This is because (i) OC association with Al may be more important than Fe under long-term waterlogged conditions in soils (Inagaki et al., 2020) and (ii) competition between Fe and Al cations to bind to functional groups of organic acids is pH driven (Hall and Thompson, 2022; Pinheiro et al., 2000). Less Al-OC complexes form at lower pH (between pH 3.5 and pH 4.5; Scheel et al., 2008; Jansen et al., 2003; Nierop et al., 2002; Schwesig et al., 2003). The soil pH at the site is significantly lower in organic horizons than in mineral horizons (4.0 \pm 0.2 and 5.2 \pm 0.6, respectively, p-value < 0.001; based on data from Mauclet et al., 2023): this likely explains the lower contribution of Al to OC complexation in the organic horizons relative to mineral horizons.

The high Ca contribution to OC complexation in the litter is likely related to plant cycling (e.g., Mauclet et al., 2022; Villani et al., 2022). The higher pH at the permafrost table or in permafrost than in surface layers (5.3 ± 0.7 and 4.0 ± 0.2 , respectively, p-value < 0.001; based on data from Mauclet et al., 2023) do not increase the Ca-complexation relative to Fe- or Al-complexation in deeper layers. This is because the

contribution of Ca to OC complexation is only expected to increase at pH >7 (Rowley et al., 2018). Nonetheless, in deep permafrost layers, Cacomplexation sometimes equals Fe-complexation, as illustrated for Mod 2 (Fig. 5c).

4.1.2. Complexation and interactions with poorly crystalline oxides contributing to mineral-associated OC

In addition to complexation, organo-mineral associations with poorly crystalline Fe oxides (i.e., ferrihydrite) might increase the overall potential for minerals to stabilize OC. Ferrihydrite minerals are highly effective sorbents characterized by a high specific surface area (200–800 $\rm m^2~g^{-1}$; Kleber et al., 2021) and are potentially present in permafrost soils which may offer additional stabilizing surfaces for OC. We assessed the overall percentage of OC out of the TOC that is mineral-bound by forming i) organo-metallic complexes and ii) organo-mineral associations.

For organo-metallic complexes, the pyrophosphate extracted carbon concentration (C_p) has been measured and can be used as an indicator of the amount of complexed carbon. The metal: C molar ratio of 0.15 for samples from this study (on average, Supplementary Material Data) suggests that functional groups of organic acids are saturated with metals. Indeed, in moist acidic tundra soils, carboxylic groups (pKa around 4-5; Stevenson, 1994) are the most common functional group of organic acids. The ratio is one functional group (i.e., the part that binds to metal ions) for 10 atoms of C, which means that with a metal:C molar ratio above 0.1, organic acids are saturated (Boudot et al., 1989; Catrouillet et al., 2014; Stevenson, 1994). The fact that organic acids are saturated with metals in the studied soils supports that OC is less available to microorganisms than if organic acids were unsaturated (Oades, 1988). In turn, the data support that the mechanism of complexation contributes to OC stability and slows down its decomposition rate (Chen et al., 2022; Kaiser and Guggenberger, 2007; Kalbitz et al., 2005).

For organo-mineral associations, we determined the concentration of poorly crystalline oxides such as ferrihydrite (Fe $_{\rm o}$ – Fe $_{\rm p}$), i.e., the most important poorly crystalline metal oxide in moist acidic tundra soils (Herndon et al., 2017). Based on literature, up to 0.22 g OC g $^{-1}$ Fe (Fe as poorly crystalline oxides) can be bound to ferrihydrite in soils (Wagai and Mayer, 2007). In this study, the data highlight that majority of poorly crystalline oxide-bound OC is in permafrost (Fig. 6; Table S2).

By adding both mechanisms (organo-metallic complexes and organomineral associations), we demonstrate that a significant proportion of TOC is potentially stabilized by these mineral OC interactions, both in permafrost and active layer soils. This can be illustrated by the poorly thawed soil profile (Min 3) displaying a range of mineral-associated TOC from 6.7% to 48% (Fig. 6b), and the deeply thawed profile (Mod 2) displaying a range between 6.5% and 59% (Fig. 6d). With the accumulation of organo-metallic complexes, the OC stored in soils at the water table level is at least 10% more mineral-bound than in the rest of the profile. The OC stabilizing potential at the water table (114 g kg $^{-1}$ of complexed C and 1.0 g kg⁻¹ of poorly crystalline oxide-bound OC) is 25%. This is a lower proportion of potential OC stabilization than observed in permafrost soils. One reason for this is that the TOC content in permafrost is lower than in active layer samples, so that any organomineral associations and metal complexation with TOC makes up a larger proportion of mineral-associated TOC.

The percentage of mineral-associated TOC (as complexation and organo-mineral associations) ranges between 6% and 59% in EML tundra soils (n = 124, mean 20%; Table S2). This falls in line with previous findings in permafrost regions from the Qinghai-Tibetan Plateau where between 1% and 59% (mean 20%) of OC is associated to Fe (after DCB extraction protocol; Mu et al., 2016; note the data can be compared given that DCB-extracted and oxalate-extracted Fe concentrations are equal in our soils). Our data support that complexation is the most abundant mechanism of mineral OC interaction in tundra soils, followed by association with poorly crystalline oxides such as ferrihydrite, and

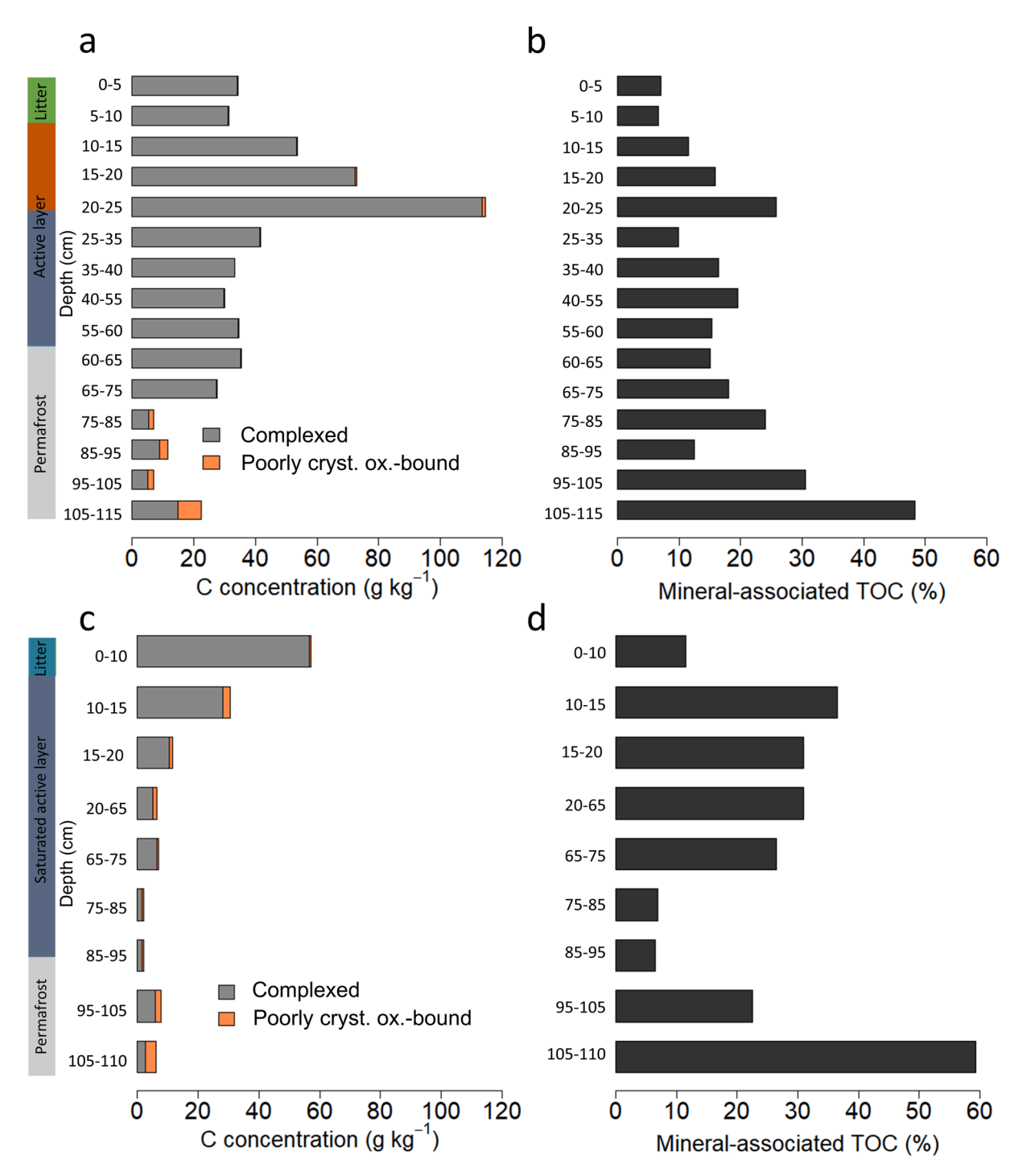


Fig. 6. For a partially unsaturated poorly thawed soil profile (Min 3; a-b) and waterlogged deeply thawed soil profile (Mod 2; c-d) profile: (a, c) Concentration of organic carbon associated with metal cations (Fe, Al, Ca and Mn) by complexation (complexed; gray) or by organo-mineral associations with poorly crystalline oxides such as ferrihydrite (poorly cryst. ox.-bound; orange) and (b, d) percentage of mineral-associated total organic carbon (TOC) (associated to poorly crystalline oxides and complexed with metals (Fe, Al, Mn and Ca)). The stratigraphic column on the left represents permafrost (gray), saturated (blue) and unsaturated (brown) active layer and litter (green).

the role of well-crystalline oxides is negligible. Scenarios to predict the evolution of mineral-associated OC upon permafrost thaw should consider the type of binding for OC given that mineral OC interactions are expected to evolve differently as a function of water saturation (Opfergelt, 2020).

4.2. Total Fe and Mn concentrations: Proxies for reactive Fe and Mn

Not all metals in soils do necessarily contribute to form mineral OC interactions. However, this study suggests that the proportion of metals that play a role in mineral OC interactions is substantial. More precisely, 76.5% of total Fe is present as a reactive form (poorly crystalline oxide or complexed) in organic samples (n=57) against 29.8% in mineral samples (n=67). For Mn, 40.7% and 19.5% of total Mn is present as a

reactive form in organic and mineral samples, respectively.

This highlights the critical need to quantify reactive metal phases (i. e., metal surfaces or cations capable of binding OC) in permafrost soils. We pointed out that on average 20% (and up to 59%) of TOC can be mineral-bound (with mineral cations and mineral surfaces). However, data from selective extractions needed to quantify the reactive mineral pool are scarce around the permafrost regions and hinder the development of a comprehensive dataset of reactive Fe which is the pool strongly involved in OC stabilization (Joss et al., 2022; Kaiser and Guggenberger, 2003; Mikutta et al., 2006; Mu et al., 2016; Patzner et al., 2020). Nonetheless, we found a high correlation between the total Fe and reactive Fe (i.e., oxalate-extracted) and similar conclusions are drawn for Mn. For both metals, these linear regressions are a function of the matrix of the sample. Mineral (TOC <20 wt%) and organic (TOC >20 wt%) samples follow different linear regressions with a high determination coefficient. For Fe, the organic samples have a $R^2 = 0.96$, and mineral samples an $R^2 = 0.84$ (Fig. 7a). For Mn, organic and mineral samples have $R^2 = 0.97$ and 0.95, respectively (Fig. 7b). No such correlations were observed for Alo and Can as function of their total concentration (not shown).

These regressions based on dry and wet tundra sites might be a useful tool to approximate the amount of reactive Fe and Mn. The reactive Fe and Mn pools are a function of the total Fe and Mn concentrations, respectively. In a large range of permafrost sites, the TOC is a commonly measured parameter, and the total concentrations in metals can be determined with minimal pre-treatment using the pXRF method providing a fast and reliable measurement (Monhonval et al., 2021b). It follows that a wider estimation of reactive Fe and Mn minerals in permafrost soils could be achieved through total Fe and Mn concentration measurements.

4.3. Mineral OC interactions hotspots

4.3.1. Hotspots of mineral OC interactions at the water table

In the active layer, we observe a marked Fe accumulation at the redox interface located at the water table, i.e., the limit between unsaturated and saturated soil layers. This accumulation is spatially narrow: only a 5-10 cm soil layer presents higher Fe concentrations (Fig. 2). The correlation between the reactive forms of Fe (oxalate- and pyrophosphate-extracted) and organics acid (ODOE and C_p) is higher (r = 0.93 and 0.84, respectively) close to the water table than further from the water table (r = 0.6 and 0.74, respectively) (Fig. 8). This is consistent with previous observations showing that redox changes can occur at

centimeter scale within flat tundra landscape characterized by poor drainage (Herndon et al., 2020; Liljedahl et al., 2011; Lipson et al., 2010; Zona et al., 2011). We hypothesize that soluble Fe²⁺ from the deep active layer migrates upward with water table fluctuations and precipitates as complexed Fe under oxic conditions (Colombo et al., 2014; Herndon et al., 2017; Lipson et al., 2012). Similar immobilization of Fe has been explained by abrupt changes in redox potential under welldrained micro-highs of polygonal tundra sites (Fiedler et al., 2004). However, the accumulation of reactive forms of Fe and organic acids disappears in waterlogged soils where no redox interface exists, i.e., when the water table is at or above soil surface (Fig. 4e and f and Fig. 6c). We demonstrate that the water table level is a transient zone for the accumulation of organic acids. It follows that fluctuations from wet to drier conditions, and more generally water table fluctuations in permafrost soils, result in the development of a hotspot where OC can be trapped.

4.3.2. Hotspots of mineral OC interactions in the permafrost

Reactive Fe in permafrost is shown to be a combination of both complexed Fe (Fe $_p$) and poorly crystalline Fe oxides (Fe $_0$ -Fe $_p$). In permafrost layers, Fe and Mn accumulation are often concomitant with TOC increase (Pond 9; Fig. S2 and Fig. S3), with some exceptions. Similar Fe accumulation in frozen peat layers has already been described in deep sediments from the ice-rich permafrost region (Monhonval et al., 2021a): in these buried peat layers, Fe accumulation was explained as a consequence of microscale oxic conditions promoted by the peat layer itself that favors Fe precipitation. Cryoturbation of surface soil could be another explanation and has been reported in this moist acidic tundra area below 1 m depth (Hutchings et al., 2019).

In organic-rich samples (TOC >20 wt%), reactive Fe is dominantly present as complexes with OC, while in mineral samples (TOC <20 wt%) reactive Fe is both in the poorly crystalline and complexed forms (Fig. 9a). Indeed, organic molecules can suppress iron oxy(hydr)oxide precipitation by complexing dissolved Fe (III) (Herndon et al., 2017; Karlsson et al., 2008; Sundman et al., 2014), and organic acids can also sorb to poorly crystalline ferrihydrite and prevent transition to more crystalline forms such as goethite or magnetite minerals (Herndon et al., 2017; Schwertmann and Murad, 1988). Ferric iron in peat soils with low pH and low Fe content (i.e., such as found in these active layer soils) tend to form mononuclear Fe(III)—OM complexes whereas in soils with high pH and high Fe content (i.e., such as found in permafrost), Fe(oxy)hydroxides are the dominant species (Karlsson et al., 2008). The poor drainage of soils can result in an overall decrease in the crystallinity of

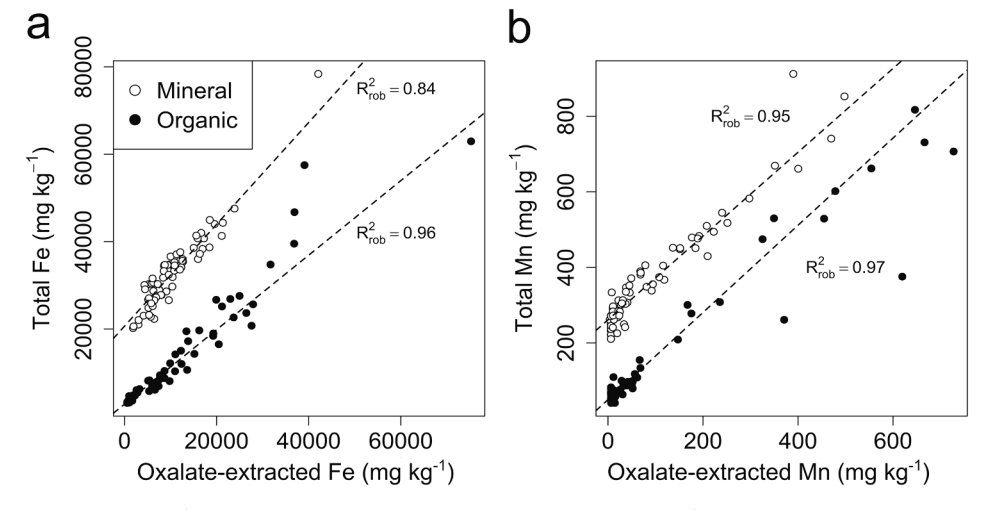


Fig. 7. Total metal concentration (in mg kg $^{-1}$) as a function of reactive (i.e., oxalate extracted; in mg kg $^{-1}$) for (a) Fe and (b) Mn in the thirteen soil profiles. Mineral samples (total organic carbon content <20%) are open circles and organic samples (total organic carbon content >20%) are full circles. Robust linear regressions are presented (dashed line, alpha = 0.95) for mineral (n = 67) and organic (n = 57) samples.

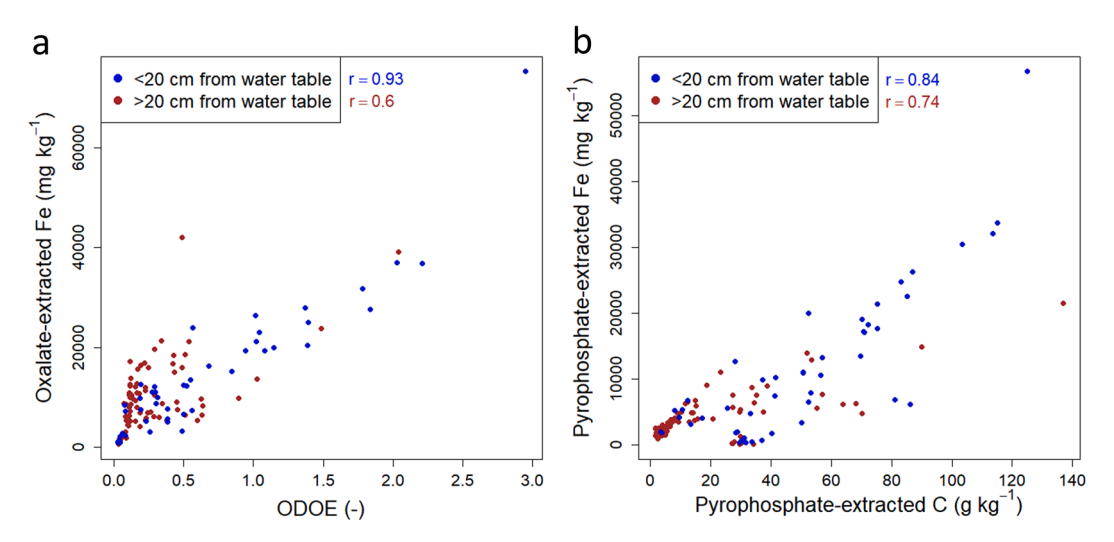


Fig. 8. In the thirteen soil profiles: (a) Oxalate-extracted Fe concentration (reactive) as function of the optical density of the oxalate extract (ODOE, adimensional), an indicator of organic acid concentration. (b) Pyrophosphate-extracted Fe concentration (complexed; $g \ kg^{-1}$) as a function of pyrophosphate-extracted C concentration (complexed; $g \ kg^{-1}$). Samples located close to the water table (<20 cm; blue) and far from the water table (>20 cm; brown) with Pearson correlation provided for both datasets (blue and brown) in panel a and b.

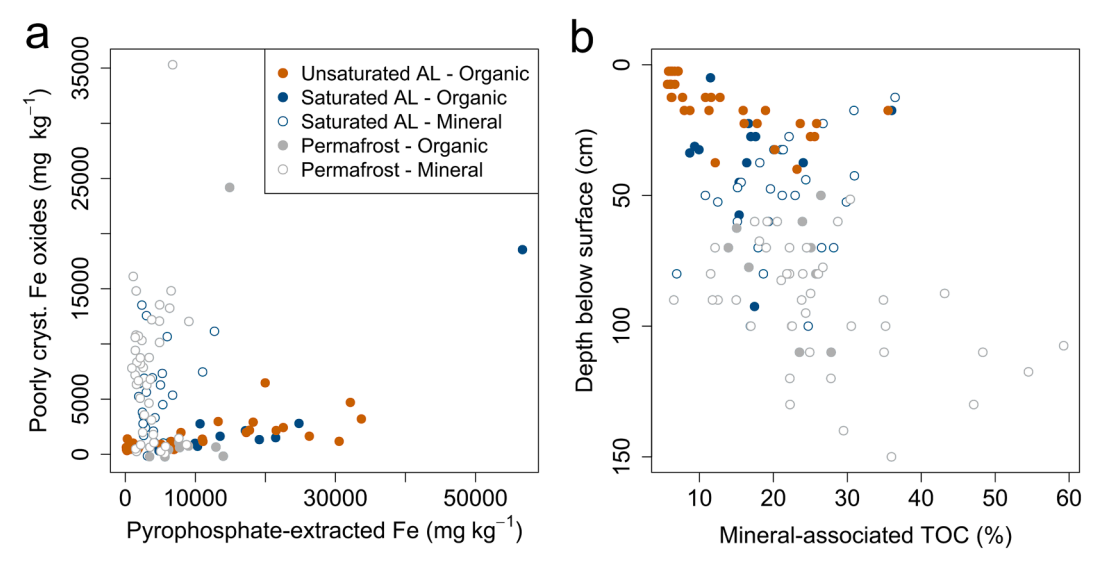


Fig. 9. In the thirteen soil profiles: (a) Concentration of Fe under poorly crystalline oxide form (difference between oxalate and pyrophosphate-extracted Fe) as a function of the concentration of pyrophosphate-extracted Fe (complexed) in the unsaturated active layer (AL, brown), saturated active layer (AL, blue) and permafrost layer (gray). (b) Percentage of mineral-associated total organic carbon (TOC) (associated to poorly crystalline oxides and complexed with metals (Fe, Al, Mn and Ca)) as a function of depth in the unsaturated active layer (brown), saturated active layer (blue) and permafrost layer (gray). The organic layers (full symbols; total organic carbon content <20%) of the soil profiles are indicated in panel a and b.

Fe oxides and promote re-crystallization as short range ordered (i.e., poorly crystalline) oxides, whereas well drained soils can present an overall increase in oxides crystallinity caused by the preferential removal of poorly crystalline oxides upon reduction (Winkler et al., 2018). In the moist acidic tundra soils from this study, the high OC content, even in mineral soils, and impeded drainage, can explain the overall absence of well crystalline oxides.

The OC in the permafrost layer is characterized by higher proportion of mineral-associated OC compared to active layer soils (p-value < 0.01; Fig. 9b). Older C as a function of depth has been reported in soils from this site (Hutchings et al., 2019). In summary, the deeper and the older the OC, the higher the proportion of mineral-associated OC (Fig. 9b). This is also confirmed by other studies related to older OC being more protected by mineral OC interactions (Grant et al., 2022; Hemingway et al., 2019; Schmidt et al., 2011; Torn et al., 1997). The proportion of mineral-associated OC ranges between 5.7 and 36% within the active

layer and between 6.5 and 59% in permafrost layers. These differences may result from soil forming processes and the duration of these processes. It is reported in this site that the OC accumulation rates are higher in the 0–66 cm layer (10.8 g OC m $^{-2}$ a $^{-1}$) compared to the 66–123 cm layer (1.4 g OC m $^{-2}$ a $^{-1}$; Hutchings et al., 2019). The active layer residence time (i.e., the time for which a soil layer is part of the active layer) is estimated to be 4.5 ka for the 0–66 cm and increases to 13.1 ka for the 66–123 cm layer (Hutchings et al., 2019). We argue that increased time under seasonal freeze-thaw cycle and above zero temperature led to an increase in the proportion of mineral-associated OC for deeper OC (currently found in permafrost layers) (Fig. 9b).

5. Conclusions

From this study we conclude that:

- (i) Between 6% and 59% of TOC (mean 20%) in Eight Mile Lake tundra soils is mineral-bound, by a combination of organomineral association (association between poorly crystalline oxides and OC) and organo-metallic complexes (associations between organic acids and Fe, Mn, Al, Ca polyvalent cations). A higher proportion of TOC is mineral-bound in permafrost layers (mean 25.4%) than in active layers (mean 16.5%).
- (ii) Mineral-bound OC is present as organo-metallic complexes in the active layer and in the permafrost, whereas organo-mineral associations are mainly found in permafrost layers. In organometallic complexes, Fe cations prevail relative to other metals (Al, Ca, Mn) except in litter (0–5 cm layer) where Ca cations are prevalent with some contribution from Mn cations. In active layer soils, complexation is dominated by Fe but the Al contribution increases under persistent waterlogged conditions.
- (iii) In these tundra soils, the proportion of reactive Fe and Mn, i.e., the proportion of Fe and Mn playing a role in mineral OC interactions, can be estimated from total Fe and Mn concentrations, respectively, with a R² better than 0.96 for organic-rich samples (>20 wt% OC) and better than 0.84 for mineral samples (<20 wt % OC).
- (iv) In the active layer, the higher pool of mineral-bound OC is found at the water table level, i.e., a redox interface where organometallic complexes dominated by Fe cations accumulate. In the permafrost, the TOC content is lower and a higher proportion of TOC is mineral-associated relative to the active layer.

Declaration of Competing Interest

The authors declare that they have no known competing financial interests or personal relationships that could have appeared to influence the work reported in this paper.

Data availability

All data are provided in the Supplementary material

Acknowledgments

The authors acknowledge the Mineral and Organic Chemical Analysis (MOCA) platform at UCLouvain conducting chemical analysis, Aubry Vandeuren and Benoît Pereira for their expertise on portable X-ray Fluorescence, Juri Palmtag, Sébastien François and the technical unit from Earth and Life Institute environment (ELIE) for their help with the steel pipe sampling device construction. We thank Simon Malvaux and Justin Ledman for their help on the field, the scientific team from the Center for Ecosystem Science and Society (ECOSS) in Flagstaff for their expertise on Eight Mile Lake study site, and the WeThaw team for insightful discussions. We acknowledge the associate editor Alberto Agnelli and two anonymous reviewers for their constructive comments. This work was supported by the European Union's Horizon 2020 research and innovation program [grant agreement No. 714617] to SO, and SO acknowledges funding from the Fund for Scientific Research FNRS in Belgium [FC69480].

Appendix A. Supplementary data

Supplementary data to this article can be found online at $\frac{\text{https:}}{\text{doi.}}$ org/10.1016/j.geoderma.2023.116552.

References

Avis, C.A., Weaver, A.J., Meissner, K.J., 2011. Reduction in areal extent of high-latitude wetlands in response to permafrost thaw. Nat. Geosci. 4, 444–448. https://doi.org/ 10.1038/ngeo1160. J.A. Baldock J.O. Skjemstad Role of the soil matrix and minerals in protecting natural organic materials against biological attack Org. Geochem. 31 2000 697 710 10.1016/S0146-6380(00)00049-8.

- Bascomb, C.L., 1968. Distribution of Pyrophosphate-Extractable Iron and Organic Carbon in Soils of Various Groups. J. Soil Sci. 19, 251–268. https://doi.org/ 10.1111/j.1365-2389.1968.tb01538.x.
- Bhattacharyya, A., Campbell, A.N., Tfaily, M.M., Lin, Y., Kukkadapu, R.K., Silver, W.L., Nico, P.S., Pett-Ridge, J., 2018a. Redox Fluctuations Control the Coupled Cycling of Iron and Carbon in Tropical Forest Soils. Environ. Sci. Technol. 52, 14129–14139. https://doi.org/10.1021/acs.est.8b03408.
- Bhattacharyya, A., Schmidt, M.P., Stavitski, E., Martínez, C.E., 2018b. Iron speciation in peats: Chemical and spectroscopic evidence for the co-occurrence of ferric and ferrous iron in organic complexes and mineral precipitates. Org. Geochem. 115, 124–137. https://doi.org/10.1016/j.orggeochem.2017.10.012.
- Blakemore, L.C., Searle, P.L., Daly, B.K., 1981. Methods for chemical analysis of soils. New Zealand Soil Bureau Scientific Report 10 A, second revision 102. https://doi. org/10.7931/DL1-SBSR-10A.
- Boudot, J.P., Bel Hadj Brahim, A., Steiman, R., Seigle-Murandi, F., 1989. Biodegradation of synthetic organo-metallic complexes of iron and aluminium with selected metal to carbon ratios. Soil Biol. Biochem. 21 (7), 961–966.
- Bring, A., Fedorova, I., Dibike, Y., Hinzman, L., Mård, J., Mernild, S.H., Prowse, T., Semenova, O., Stuefer, S.L., Woo, M.-K., 2016. Arctic terrestrial hydrology: A synthesis of processes, regional effects, and research challenges: Arctic Terrestrial Hydrology. J. Geophys. Res. Biogeosciences 121, 621–649. https://doi.org/10.1002/2015JG003131.
- Brown, J., Ferrians, O.J., Heginbottom, J.A., Melnikov, E.S., Akerman, J., 1998. Circum-Arctic map of permafrost and ground-ice conditions. Circum-Pacific Map Series CP-45, scale 1:10,000,000, Tech. rep., U.S.Geological Survey in Cooperation with the Circum-Pacific Council for Energy and Mineral Resources.
- Catrouillet, C., Davranche, M., Dia, A., Bouhnik-Le Coz, M., Marsac, R., Pourret, O., Gruau, G., 2014. Geochemical modeling of Fe(II) binding to humic and fulvic acids. Chem. Geol. 372, 109–118. https://doi.org/10.1016/j.chemgeo.2014.02.019.
- Chao, T.T., Sanzolone, R.F., 1992. Decomposition techniques. J. Geochem. Explor. 44 (1-3), 65–106.
- Chen, Q., Zhang, P., Hu, Z., Li, S., Zhang, Y., Hu, L., Zhou, L., Lin, B., Li, X., 2022. Soil Organic Carbon and Geochemical Characteristics on Different Rocks and Their Significance for Carbon Cycles. Front. Environ, Sci, p. 9.
- Colombo, C., Palumbo, G., He, J.-Z., Pinton, R., Cesco, S., 2014. Review on iron availability in soil: interaction of Fe minerals, plants, and microbes. J. Soils Sediments 14, 538–548. https://doi.org/10.1007/s11368-013-0814-z.
- Daly, B.K., 1982. Identification of podzols and podzolised soils in New Zealand by relative absorbance of oxalate extracts of A and B horizons. Geoderma 28, 29–38. https://doi.org/10.1016/0016-7061(82)90038-6.
- Eglinton, T.I., 2012. A rusty carbon sink. Nature 483, 165–166. https://doi.org/10.1038/
- Eusterhues, K., Rumpel, C., Kögel-Knabner, I., 2005. Organo-mineral associations in sandy acid forest soils: importance of specific surface area, iron oxides and micropores. Eur. J. Soil Sci. 56, 753–763. https://doi.org/10.1111/j.1365-2389.2005.00710.x.
- Fiedler, S., Sommer, M., 2004. Water and Redox Conditions in Wetland Soils—Their Influence on Pedogenic Oxides and Morphology. SOIL SCI SOC AM J 68 (1), 326–335.
- Fiedler, S., Wagner, D., Kutzbach, L., Pfeiffer, E.-M., 2004. Element Redistribution along Hydraulic and Redox Gradients of Low-Centered Polygons, Lena Delta, Northern Siberia. Soil Sci. Soc. Am. J. 68, 1002–1011. https://doi.org/10.2136/ sssai2004.1002.
- Garnello, A., Marchenko, S., Nicolsky, D., Romanovsky, V., Ledman, J., Celis, G., Schädel, C., Luo, Y., Schuur, E. a. G., 2021. Projecting Permafrost Thaw of Sub-Arctic Tundra With a Thermodynamic Model Calibrated to Site Measurements. J. Geophys. Res. Biogeosciences 126, e2020JG006218. https://doi.org/10.1029/ 2020JG006218.
- Grant, K.E., Galy, V.V., Haghipour, N., Eglinton, T.I., Derry, L.A., 2022. Persistence of old soil carbon under changing climate: The role of mineral-organic matter interactions. Chem. Geol. 587, 120629 https://doi.org/10.1016/j.chemgeo.2021.120629.
- Hall, S.J., Thompson, A., 2022. What do relationships between extractable metals and soil organic carbon concentrations mean? Soil Sci. Soc. Am. J. 86, 195–208. https:// doi.org/10.1002/saj2.20343.
- Hemingway, J.D., Rothman, D.H., Grant, K.E., Rosengard, S.Z., Eglinton, T.I., Derry, L.A., Galy, V.V., 2019. Mineral protection regulates long-term global preservation of natural organic carbon. Nature 570, 228–231. https://doi.org/10.1038/s41586-019-1280-6.
- Herndon, E., AlBashaireh, A., Singer, D., Roy Chowdhury, T., Gu, B., Graham, D., 2017. Influence of iron redox cycling on organo-mineral associations in Arctic tundra soil. Geochim. Cosmochim. Acta 207, 210–231. https://doi.org/10.1016/j. gca.2017.02.034.
- Herndon, E., Kinsman-Costello, L., Godsey, S., 2020. Biogeochemical Cycling of Redox-Sensitive Elements in Permafrost-Affected Ecosystems, in: Dontsova, K., Balogh-Brunstad, Z., Le Roux, G. (Eds.), Geophysical Monograph Series. Wiley, pp. 245–265. https://doi.org/10.1002/9781119413332.ch12.
- Hirst, C., Mauclet, E., Monhonval, A., Tihon, E., Ledman, J., Schuur, E.A.G., Opfergelt, S., 2022. Seasonal Changes in Hydrology and Permafrost Degradation Control Mineral Element-Bound DOC Transport From Permafrost Soils to Streams. Glob. Biogeochem. Cycles 36, e2021GB007105. https://doi.org/10.1029/2021GB007105.
- Hugelius, G., Strauss, J., Zubrzycki, S., Harden, J.W., Schuur, E.A.G., Ping, C.-L., Schirrmeister, L., Grosse, G., Michaelson, G.J., Koven, C.D., O'Donnell, J.A., Elberling, B., Mishra, U., Camill, P., Yu, Z., Palmtag, J., Kuhry, P., 2014. Estimated

- stocks of circumpolar permafrost carbon with quantified uncertainty ranges and identified data gaps. Biogeosciences 11 (23), 6573–6593.
- Hutchings, J.A., Bianchi, T.S., Kaufman, D.S., Kholodov, A.L., Vaughn, D.R., Schuur, E.A. G., 2019. Millennial-scale carbon accumulation and molecular transformation in a permafrost core from Interior Alaska. Geochim. Cosmochim. Acta 253, 231–248. https://doi.org/10.1016/j.gca.2019.03.028.
- Inagaki, T.M., Possinger, A.R., Grant, K.E., Schweizer, S.A., Mueller, C.W., Derry, L.A., Lehmann, J., Kögel-Knabner, I., 2020. Subsoil organo-mineral associations under contrasting climate conditions. Geochim. Cosmochim. Acta 270, 244–263. https://doi.org/10.1016/j.gca.2019.11.030.
- IPCC, 2021. Summary for Policymakers. In: Climate Change 2021: The Physical Science Basis. Contribution of Working Group I to the Sixth Assessment Report of the Intergovernmental Panel on Climate Change [Masson-Delmotte, V., P. Zhai, A. Pirani, S. L. Connors, C. Péan, S. Berger, N. Caud, Y. Chen, L. Goldfarb, M. I. Gomis, M. Huang, K. Leitzell, E. Lonnoy, J.B.R. Matthews, T. K. Maycock, T. Waterfield, O. Yelekçi, R. Yu and B. Zhou (eds.)]. Cambridge University Press. In Press.
- IUSS Working Group WRB, 2015. World Reference Base for Soil Resources 2014, update 2015 International soil classification system for naming soils and creating legends for soil maps. World Soil Resour. Rep.
- Jansen, B., Nierop, K.G., Verstraten, J.M., 2003. Mobility of Fe(II), Fe(III) and Al in acidic forest soils mediated by dissolved organic matter: influence of solution pH and metal/organic carbon ratios. Geoderma 113, 323–340. https://doi.org/10.1016/ S0016-7061(02)00368-3.
- Jobbágy, E.G., Jackson, R.B., 2004. The Uplift of Soil Nutrients by Plants: Biogeochemical Consequences Across Scales. Ecology 85, 2380–2389. https://doi. org/10.1890/03-0245.
- Joss, H., Patzner, M.S., Maisch, M., Mueller, C.W., Kappler, A., Bryce, C., 2022. Cryoturbation impacts iron-organic carbon associations along a permafrost soil chronosequence in northern Alaska. Geoderma 413, 115738. https://doi.org/ 10.1016/j.geoderma.2022.115738.
- Kaiser, K., Guggenberger, G., 2003. Mineral surfaces and soil organic matter. Eur. J. Soil Sci. 54, 219–236. https://doi.org/10.1046/j.1365-2389.2003.00544.x.
- Kaiser, K., Guggenberger, G., 2007. Sorptive stabilization of organic matter by microporous goethite: sorption into small pores vs. surface complexation. Eur. J. Soil Sci. 58, 45–59. https://doi.org/10.1111/j.1365-2389.2006.00799.x.
- Kaiser, K., Guggenberger, G., Haumaier, L., Zech, W., 1997. Dissolved organic matter sorption on sub soils and minerals studied by 13C-NMR and DRIFT spectroscopy. Eur. J. Soil Sci. 48, 301–310. https://doi.org/10.1111/j.1365-2389.1997.tb00550.x.
- Kalbitz, K., Kaiser, K., 2008. Contribution of dissolved organic matter to carbon storage in forest mineral soils. J. Plant Nutr. Soil Sci. 171, 52–60. https://doi.org/10.1002/ ipln 200700043
- Kalbitz, K., Schwesig, D., Rethemeyer, J., Matzner, E., 2005. Stabilization of dissolved organic matter by sorption to the mineral soil. Soil Biol. Biochem. 37, 1319–1331. https://doi.org/10.1016/j.soilbio.2004.11.028.
- Karlsson, T., Persson, P., Skyllberg, U., Mörth, C.-M., Giesler, R., 2008. Characterization of Iron(III) in Organic Soils Using Extended X-ray Absorption Fine Structure Spectroscopy. Environ. Sci. Technol. 42, 5449–5454. https://doi.org/10.1021/es800322i
- Kelley, A.K., Pegoraro, E., Mauritz, M., Hutchings, J., Natali, S., Hicks-Pries, C.E., Schuur, E., Bonanza Creek LTER, 2022. Eight Mile Lake Research Watershed, Thaw Gradient: Seasonal thaw depth 2004-2021. Bonanza Creek LTER University of Alaska Fairbanks. BNZ:519, http://www.lter.uaf.edu/data/data-detail/id/519. https://doi.org/10.6073/pasta/854b92439ccceec557a810d09dfaf174.
- Kleber, M., Eusterhues, K., Keiluweit, M., Mikutta, C., Mikutta, R., Nico, P.S., 2015. Mineral-Organic Associations: Formation, Properties, and Relevance in Soil Environments, in: Advances in Agronomy. Elsevier, pp. 1–140. https://doi.org/ 10.1016/bs.agron.2014.10.005.
- Kleber, M., Bourg, I.C., Coward, E.K., Hansel, C.M., Myneni, S.C.B., Nunan, N., 2021. Dynamic interactions at the mineral-organic matter interface. Nat. Rev. Earth Environ. https://doi.org/10.1038/s43017-021-00162-y.
- Kögel-Knabner, I., Amelung, W., Cao, Z., Fiedler, S., Frenzel, P., Jahn, R., Kalbitz, K., Kölbl, A., Schloter, M., 2010. Biogeochemistry of paddy soils. Geoderma 157, 1–14. https://doi.org/10.1016/j.geoderma.2010.03.009.
- Lalonde, K., Mucci, A., Ouellet, A., Gélinas, Y., 2012. Preservation of organic matter in sediments promoted by iron. Nature 483, 198–200. https://doi.org/10.1038/ nature10855.
- Lenton, T.M., Rockström, J., Gaffney, O., Rahmstorf, S., Richardson, K., Steffen, W., Schellnhuber, H.J., 2019. Climate tipping points — too risky to bet against. Nature 575, 592–595. https://doi.org/10.1038/d41586-019-03595-0.
- Li, H., Santos, F., Butler, K., Herndon, E., 2021. A Critical Review on the Multiple Roles of Manganese in Stabilizing and Destabilizing Soil Organic Matter. Environ. Sci. Technol. 55, 12136–12152. https://doi.org/10.1021/acs.est.1c00299.
- Liljedahl, A.K., Hinzman, L.D., Harazono, Y., Zona, D., Tweedie, C.E., Hollister, R.D., Engstrom, R., Oechel, W.C., 2011. Nonlinear controls on evapotranspiration in arctic coastal wetlands. Biogeosciences 8, 3375–3389. https://doi.org/10.5194/bg-8-2375-2011
- Lim, A.G., Loiko, S.V., Kuzmina, D.M., Krickov, I.V., Shirokova, L.S., Kulizhsky, S.P., Pokrovsky, O.S., 2022. Organic carbon, and major and trace elements reside in labile low-molecular form in the ground ice of permafrost peatlands: a case study of colloids in peat ice of Western Siberia. Environ. Sci.: Processes Impacts 24 (9), 1443–1459.
- Lipson, D.A., Jha, M., Raab, T.K., Oechel, W.C., 2010. Reduction of iron (III) and humic substances plays a major role in anaerobic respiration in an Arctic peat soil. J. Geophys. Res. 115, G00I06. https://doi.org/10.1029/2009JG001147.
- Lipson, D.A., Zona, D., Raab, T.K., Bozzolo, F., Mauritz, M., Oechel, W.C., 2012. Water-table height and microtopography control biogeochemical cycling in an Arctic

- coastal tundra ecosystem. Biogeosciences 9, 577–591. https://doi.org/10.5194/bg-9-577-2012.
- Luo, D., Wu, Q., Jin, H., Marchenko, S.S., Lü, L., Gao, S., 2016. Recent changes in the active layer thickness across the northern hemisphere. Environ. Earth Sci. 75, 555. https://doi.org/10.1007/s12665-015-5229-2.
- Masiello, C.A., Chadwick, O.A., Southon, J., Torn, M.S., Harden, J.W., 2004. Weathering controls on mechanisms of carbon storage in grassland soils. Glob. Biogeochem. Cycles 18 (4).
- Mauclet, E., Agnan, Y., Hirst, C., Monhonval, A., Pereira, B., Vandeuren, A., Villani, M., Ledman, J., Taylor, M., Jasinski, B.L., Schuur, E.A.G., Opfergelt, S., 2022. Changing sub-Arctic tundra vegetation upon permafrost degradation: impact on foliar mineral element cycling. Biogeosciences 19, 2333–2351. https://doi.org/10.5194/bg-19-2333-2022
- Mauclet, E., Hirst, C., Monhonval, A., Stevenson, E.I., Gérard, M., Villani, M., Dailly, H., Schuur, E.A.G., Opfergelt, S., 2023. Tracing changes in base cation sources for Arctic tundra vegetation upon permafrost thaw. Geoderma 429, 116277. https://doi.org/ 10.1016/j.geoderma.2022.116277.
- Mauritz, M., Bracho, R., Celis, G., Hutchings, J., Natali, S.M., Pegoraro, E., Salmon, V.G., Schädel, C., Webb, E.E., Schuur, E.A.G., 2017. Nonlinear CO2 flux response to 7 years of experimentally induced permafrost thaw. Glob. Change Biol. 23, 3646–3666. https://doi.org/10.1111/gcb.13661.
- Mehra, O.P., Jackson, M.L., 1960. Iron oxide removal from soils and clays by a dithionite-citrate system buffered with sodium bicarbonate. Clays Clay Miner. 317–327 https://doi.org/10.1016/B978-0-08-009235-5.50026-7.
- Mikutta, R., Kleber, M., Torn, M.S., Jahn, R., 2006. Stabilization of Soil Organic Matter: Association with Minerals or Chemical Recalcitrance? Biogeochemistry 77, 25–56. https://doi.org/10.1007/s10533-005-0712-6.
- Mikutta, R., Mikutta, C., Kalbitz, K., Scheel, T., Kaiser, K., Jahn, R., 2007. Biodegradation of forest floor organic matter bound to minerals via different binding mechanisms. Geochim. Cosmochim. Acta 71, 2569–2590. https://doi.org/10.1016/j. gca.2007.03.002.
- Monhonval, A., Mauclet, E., Pereira, B., Vandeuren, A., Strauss, J., Grosse, G., Schirrmeister, L., Fuchs, M., Kuhry, P., Opfergelt, S., 2021a. Mineral Element Stocks in the Yedoma Domain: A Novel Method Applied to Ice-Rich Permafrost Regions. Front. Earth Sci. 9, 773. https://doi.org/10.3389/feart.2021.703304.
- Monhonval, A., Strauss, J., Mauclet, E., Hirst, C., Bemelmans, N., Grosse, G., Schirrmeister, L., Fuchs, M., Opfergelt, S., 2021b. Iron Redistribution Upon Thermokarst Processes in the Yedoma Domain. Front. Earth Sci. 9, 629. https://doi. org/10.3389/feart.2021.703339.
- Mu, C.C., Zhang, T.J., Zhao, Q., Guo, H., Zhong, W., Su, H., Wu, Q.B., 2016. Soil organic carbon stabilization by iron in permafrost regions of the Qinghai-Tibet Plateau. Geophys. Res. Lett. 43, 10286–10294. https://doi.org/10.1002/2016GL070071.
- Natali, S.M., Schuur, E.A.G., Trucco, C., Hicks Pries, C.E., Crummer, K.G., Baron Lopez, A.F., 2011. Effects of experimental warming of air, soil and permafrost on carbon balance in Alaskan tundra: WARMING OF ALASKAN TUNDRA. Glob. Change Biol. 17, 1394–1407. https://doi.org/10.1111/j.1365-2486.2010.02303.x.
- Nierop, K.G.J., Jansen, B., Verstraten, J.M., 2002. Dissolved organic matter, aluminium and iron interactions: precipitation induced by metalycarbon ratio, pH and competition. Sci, Total Environ, p. 11.
- Oades, J.M., 1988. The retention of organic matter in soils. Biogeochemistry 5, 35–70. $\label{eq:biogeochemistry} https://doi.org/10.1007/BF02180317.$
- Obu, J., Westermann, S., Bartsch, A., Berdnikov, N., Christiansen, H.H., Dashtseren, A., Delaloye, R., Elberling, B., Etzelmüller, B., Kholodov, A., Khomutov, A., Kääb, A., Leibman, M.O., Lewkowicz, A.G., Panda, S.K., Romanovsky, V., Way, R.G., Westergaard-Nielsen, A., Wu, T., Yamkhin, J., Zou, D., 2019. Northern Hemisphere permafrost map based on TTOP modelling for 2000–2016 at 1 km2 scale. Earth-Sci. Rev. 193, 299–316. https://doi.org/10.1016/j.earscirev.2019.04.023.
- Opfergelt, S., 2020. The next generation of climate model should account for the evolution of mineral-organic interactions with permafrost thaw. Environ. Res. Lett. 15 (9), 091003.
- Osterkamp, T.E., Romanovsky, V.E., 1999. Evidence for warming and thawing of discontinuous permafrost in Alaska. Permafr. Periglac. Process. 10, 17–37. https://doi.org/10.1002/(SICI)1099-1530(199901/03)10:1<17::AID-PPP303>3.0.CO;2-4.
- Osterkamp, T.E., Jorgenson, M.T., Schuur, E.A.G., Shur, Y.L., Kanevskiy, M.Z., Vogel, J. G., Tumskoy, V.E., 2009. Physical and ecological changes associated with warming permafrost and thermokarst in Interior Alaska. Permafr. Periglac. Process. 20, 235–256. https://doi.org/10.1002/ppp.656.
- Pan, Y., Koopmans, G.F., Bonten, L.T.C., Song, J., Luo, Y., Temminghoff, E.J.M., Comans, R.N.J., 2014. Influence of pH on the redox chemistry of metal (hydr)oxides and organic matter in paddy soils. J. Soils Sediments 14, 1713–1726. https://doi. org/10.1007/s11368-014-0919-z.
- Parfitt, R.L., Childs, C.W., 1988. Estimation of forms of Fe and Al a review, and analysis of contrasting soils by dissolution and Mossbauer methods. Soil Res. 26, 121–144. https://doi.org/10.1071/sr9880121.
- Parkinson, R.J., 1978. Genesis and classification of arctic coastal plain soils, Prudhoe Bay. Institute of Polar Studies, The Ohio State University, Alaska.
- Patzner, M.S., Mueller, C.W., Malusova, M., Baur, M., Nikeleit, V., Scholten, T., Hoeschen, C., Byrne, J.M., Borch, T., Kappler, A., Bryce, C., 2020. Iron mineral dissolution releases iron and associated organic carbon during permafrost thaw. Nat. Commun. 11, 6329. https://doi.org/10.1038/s41467-020-20102-6.
- Ping, C.-L., Michaelson, G.J., Kimble, J.M., Walker, D.A., 2005. Soil Acidity and Exchange Properties of Cryogenic Soils in Arctic Alaska. Soil Sci. Plant Nutr. 51, 649–653. https://doi.org/10.1111/j.1747-0765.2005.tb00083.x.
- Pinheiro, J.P., Mota, A.M., Benedetti, M.F., 2000. Effect of Aluminum Competition on Lead and Cadmium Binding to Humic Acids at Variable Ionic Strength. Environ. Sci. Technol. 34, 5137–5143. https://doi.org/10.1021/es0000899.

- R Core Team, 2018. R: A language and environment for statistical computing. R
 Foundation for Statistical Computing, Vienna, Austria https://www.R-project.org/-
- Ravansari, R., Lemke, L.D., 2018. Portable X-ray fluorescence trace metal measurement in organic rich soils: pXRF response as a function of organic matter fraction. Geoderma 319, 175–184. https://doi.org/10.1016/j.geoderma.2018.01.011.
- Ravansari, R., Wilson, S.C., Tighe, M., 2020. Portable X-ray fluorescence for environmental assessment of soils: Not just a point and shoot method. Environ. Int. 134, 105250 https://doi.org/10.1016/j.envint.2019.105250.
- Rennert, T., 2019. Wet-chemical extractions to characterise pedogenic Al and Fe species
 a critical review. Soil Res. 57, 1. https://doi.org/10.1071/SR18299.
- Riedel, T., Zak, D., Biester, H., Dittmar, T., 2013. Iron traps terrestrially derived dissolved organic matter at redox interfaces. Proc. Natl. Acad. Sci. 110, 10101–10105. https:// doi.org/10.1073/pnas.1221487110.
- Rowley, M.C., Grand, S., Verrecchia, É.P., 2018. Calcium-mediated stabilisation of soil organic carbon. Biogeochemistry 137, 27–49. https://doi.org/10.1007/s10533-017-0410-1
- Schaedel, C., Rodenhizer, H.G., Celis, G., Ledman, J., Schuur, E., Bonanza Creek LTER, 2022. Eight Mile Lake Research Watershed, Thaw Gradient: Seasonal water table depth from 2004-2021. Bonanza Creek LTER University of Alaska Fairbanks. BNZ: 564, http://www.lter.uaf.edu/data/data-detail/id/564. https://doi.org/10.6073/pasta/854cb809639b3173dfb2c9f2ee098f98.
- Scheel, T., Jansen, B., Van Wijk, A.J., Verstraten, J.M., Kalbitz, K., 2008. Stabilization of dissolved organic matter by aluminium: a toxic effect or stabilization through precipitation? Eur. J. Soil Sci. 59, 1122–1132. https://doi.org/10.1111/j.1365-2389.2008.01074.x.
- Schmidt, M.W.I., Torn, M.S., Abiven, S., Dittmar, T., Guggenberger, G., Janssens, I.A., Kleber, M., Kögel-Knabner, I., Lehmann, J., Manning, D.A.C., Nannipieri, P., Rasse, D.P., Weiner, S., Trumbore, S.E., 2011. Persistence of soil organic matter as an ecosystem property. Nature 478, 49–56. https://doi.org/10.1038/nature10386.
- Schuur, E.A.G., Crummer, K.G., Vogel, J.G., Mack, M.C., 2007. Plant Species Composition and Productivity following Permafrost Thaw and Thermokarst in Alaskan Tundra. Ecosystems 10, 280–292. https://doi.org/10.1007/s10021-007-9024-0.
- Schuur, E.A.G., Bockheim, J., Canadell, J.G., Euskirchen, E., Field, C.B., Goryachkin, S. V., Hagemann, S., Kuhry, P., Lafleur, P.M., Lee, H., Mazhitova, G., Nelson, F.E., Rinke, A., Romanovsky, V.E., Shiklomanov, N., Tarnocai, C., Venevsky, S., Vogel, J. G., Zimov, S.A., 2008. Vulnerability of Permafrost Carbon to Climate Change: Implications for the Global Carbon Cycle. BioScience 58, 701–714. https://doi.org/10.1641/B580807.
- Schuur, E.A.G., Vogel, J.G., Crummer, K.G., Lee, H., Sickman, J.O., Osterkamp, T.E., 2009. The effect of permafrost thaw on old carbon release and net carbon exchange from tundra. Nature 459, 556–559. https://doi.org/10.1038/nature08031.
- Schuur, E.A.G., Abbott, B.W., Bowden, W.B., Brovkin, V., Camill, P., Canadell, J.G., Chanton, J.P., Chapin, F.S., Christensen, T.R., Ciais, P., Crosby, B.T., Czimczik, C.I., Grosse, G., Harden, J., Hayees, D.J., Hugelius, G., Jastrow, J.D., Jones, J.B., Kleinen, T., Koven, C.D., Krinner, G., Kuhry, P., Lawrence, D.M., McGuire, A.D., Natali, S.M., O'Donnell, J.A., Ping, C.L., Riley, W.J., Rinke, A., Romanovsky, V.E., Sannel, A.B.K., Schädel, C., Schaefer, K., Sky, J., Subin, Z.M., Tarnocai, C., Turetsky, M.R., Waldrop, M.P., Walter Anthony, K.M., Wickland, K.P., Wilson, C.J., Zimov, S.A., 2013. Expert assessment of vulnerability of permafrost carbon to climate change. Clim. Change 119 (2), 359–374.
- E.A.G. Schuur R. Bracho G. Celis E.F. Belshe C. Ebert J. Ledman M. Mauritz E.F. Pegoraro C. Plaza H. Rodenhizer V. Romanovsky C. Schädel D. Schirokauer M. Taylor J.G. Vogel E.E. Webb Tundra Underlain By Thawing Permafrost Persistently Emits Carbon to the Atmosphere Over 15 Years of Measurements. J. Geophys. Res Biogeosciences 126 2021 e2020JG006044 10.1029/2020JG006044.
- Schuur, E.A.G., McGuire, A.D., Schädel, C., Grosse, G., Harden, J.W., Hayes, D.J., Hugelius, G., Koven, C.D., Kuhry, P., Lawrence, D.M., Natali, S.M., Olefeldt, D., Romanovsky, V.E., Schaefer, K., Turetsky, M.R., Treat, C.C., Vonk, J.E., 2015. Climate change and the permafrost carbon feedback. Nature 520, 171–179. https://doi.org/10.1038/nature14338.

- Schwertmann, U., Murad, E., 1988. The nature of an iron oxide—organic iron association in a peaty environment. Clay Miner. 23, 291–299. https://doi.org/10.1180/ claymin.1988.023.3.06.
- Schwesig, D., Kalbitz, K., Matzner, E., 2003. Effects of aluminium on the mineralization of dissolved organic carbon derived from forest floors. Eur. J. Soil Sci. 54, 311–322. https://doi.org/10.1046/j.1365-2389.2003.00523.x.
- Stevenson, F.J., 1994. Humus chemistry: genesis, composition, reactions. John Wiley & Sons.
- Strauss, J., Schirrmeister, L., Grosse, G., Fortier, D., Hugelius, G., Knoblauch, C., Romanovsky, V., Schädel, C., Schneider von Deimling, T., Schuur, E.A.G., Shmelev, D., Ulrich, M., Veremeeva, A., 2017. Deep Yedoma permafrost: A synthesis of depositional characteristics and carbon vulnerability. Earth-Sci. Rev. 172, 75–86. https://doi.org/10.1016/j.earscirev.2017.07.007.
- Street, L.E., Dean, J.F., Billett, M.F., Baxter, R., Dinsmore, K.J., Lessels, J.S., Subke, J.-A., Tetzlaff, D., Wookey, P.A., 2016. Redox dynamics in the active layer of an Arctic headwater catchment; examining the potential for transfer of dissolved methane from soils to stream water. J. Geophys. Res. Biogeosciences 121, 2776–2792. https://doi.org/10.1002/2016JG003387.
- Stumm, W., 1992. Chemistry of the solid-water interface: processes at the mineral-water and particle-water interface in natural systems.
- Sundman, A., Karlsson, T., Laudon, H., Persson, P., 2014. XAS study of iron speciation in soils and waters from a boreal catchment. Chem. Geol. 364, 93–102. https://doi.org/ 10.1016/j.chemgeo.2013.11.023
- Swindles, G.T., Morris, P.J., Mullan, D., Watson, E.J., Turner, T.E., Roland, T.P., Amesbury, M.J., Kokfelt, U., Schoning, K., Pratte, S., Gallego-Sala, A., Charman, D.J., Sanderson, N., Garneau, M., Carrivick, J.L., Woulds, C., Holden, J., Parry, L., Galloway, J.M., 2016. The long-term fate of permafrost peatlands under rapid climate warming, Sci. Rep. 5, 17951. https://doi.org/10.1038/srep17951.
- Torn, M.S., Trumbore, S.E., Chadwick, O.A., Vitousek, P.M., Hendricks, D.M., 1997. Mineral control of soil organic carbon storage and turnover. Nature 389, 170–173. https://doi.org/10.1038/38260.
- Villani, M., Mauclet, E., Agnan, Y., Druel, A., Jasinski, B., Taylor, M., Schuur, E.A.G., Opfergelt, S., 2022. Mineral element recycling in topsoil following permafrost degradation and a vegetation shift in sub-Arctic tundra. Geoderma 421, 115915.
- von Lützow, M., Kogel-Knabner, I., Ekschmitt, K., Matzner, E., Guggenberger, G., Marschner, B., Flessa, H., 2006. Stabilization of organic matter in temperate soils: mechanisms and their relevance under different soil conditions - a review. Eur. J. Soil Sci. 57, 426–445. https://doi.org/10.1111/j.1365-2389.2006.00809.x.
- Vonk, J.E., Tank, S.E., Walvoord, M.A., 2019. Integrating hydrology and biogeochemistry across frozen landscapes. Nat. Commun. 10, 5377. https://doi.org/ 10.1038/s41467-019-13361-5.
- Wagai, R., Mayer, L.M., 2007. Sorptive stabilization of organic matter in soils by hydrous iron oxides. Geochim. Cosmochim. Acta 71, 25–35. https://doi.org/10.1016/j. gca.2006.08.047.
- Wang, X., Toner, B.M., Yoo, K., 2019. Mineral vs. organic matter supply as a limiting factor for the formation of mineral-associated organic matter in forest and agricultural soils. Sci. Total Environ. 692, 344–353. https://doi.org/10.1016/j. scitotenv.2019.07.219
- Wang, D., Zang, S., Wu, X., Ma, D., Li, M., Chen, Q., Liu, X., Zhang, N., 2021. Soil organic carbon stabilization in permafrost peatlands. Saudi J. Biol. Sci. 28, 7037–7045. https://doi.org/10.1016/j.sjbs.2021.07.088.
- Winkler, P., Kaiser, K., Thompson, A., Kalbitz, K., Fiedler, S., Jahn, R., 2018. Contrasting evolution of iron phase composition in soils exposed to redox fluctuations. Geochim. Cosmochim. Acta 235, 89–102. https://doi.org/10.1016/j.gca.2018.05.019.
- Zhang, T., Barry, R., Knowles, K., Heginbottom, J.A., Brown, J., 1999. Statistics and characteristics of permafrost and ground-ice distribution in the Northern Hemisphere. Polar Geography 23, 132–154. https://doi.org/10.1080/ 10889370802175895.
- Zimov, S.A., Schuur, E.A.G., Chapin, F.S., 2006. Climate Change: Permafrost and the Global Carbon Budget. Science 312 (5780), 1612–1613.
- Zona, D., Lipson, D.A., Zulueta, R.C., Oberbauer, S.F., Oechel, W.C., 2011.
 Microtopographic controls on ecosystem functioning in the Arctic Coastal Plain.
 J. Geophys. Res. 116, G00I08. https://doi.org/10.1029/2009JG001241.